國　立　交　通　大　學

電信工程學系碩士班

碩士論文

WCDMA 蜂巢式系統中提供多速率服務之類神經模糊呼叫允諾控制

Neural Fuzzy Call Admission Control for WCDMA Cellular Systems Providing Multirate Services

研 究 生：郭立忠

指導教授：張仲儒　教授

中華民國九十四年六月

WCDMA 蜂巢式系統中提供多速率服務之類神經模糊呼叫允諾控制

Neural Fuzzy Call Admission Control for WCDMA Cellular Systems Providing Multirate Services

研 究 生：郭立忠　　Student: Li-Chung Kuo

指導教授：張仲儒　教授　　Advisor: Dr. Chung-Ju Chang

國立交通大學

電信工程學系碩士班

碩士論文

A Thesis

Submitted to Institute of Communication Engineering

College of Electrical Engineering and Computer Science

National Chiao Tung University

in Partial Fulfillment of the Requirements

for the Degree of Master of Science

in

Electrical Engineering

June 2005

Hsinchu, Taiwan, Republic of China

中華民國九十四年六月

WCDMA 蜂巢式系統中提供多速率服務之類神經乏晰呼叫允諾控制

研究生：郭立忠　　指導教授：張仲儒 教授

國立交通大學電信工程學系碩士班

中文摘要

寬頻分碼多工擷取(WCDMA)的技術，應用在第三代行動通訊(3G)的時代裡。許多企業投入大量資金以及人力在研發 WCDMA 蜂巢式系統，祈望能使得通訊系統更有效率。為了達到此目的，要設計一套合適的呼叫允諾控制方法，才能改善效能並且保障系統的服務品質。由此可知，設計 WCDMA 呼叫允諾控制方法對於通訊系統是相當重要的。我們提出一套類神經乏晰呼叫允諾以及傳輸速率控制(NFCAC-RC)的方法，經由考慮系統的通訊中斷率、預測的系統干擾量、使用者對周遭通訊的影響，NFCAC-RC 可以保障系統的服務品質，並且提高系統的使用率。

再者，我們考慮不同形式的資料使用者對系統的影響。當系統充斥著傳輸大量資料的使用者時，要保障系統的服務品質就不是一件容易的事。NFCAC-RC 採用控制傳輸速率的方法來克服這種情況，而模擬的結果也顯示 NFCAC-RC 能夠有效的提升系統的效能。

Neural Fuzzy Call Admission Control for WCDMA Cellular Systems Providing Multirate Services

Student: Li-Chung Kuo Advisor: Dr. Chung-Ju Chang

Institute of Communication Engineering
National Chiao Tung University

Abstract

Wideband code division multiple access (WCDMA) is used as a radio interface for the third generation (3G) mobile systems. Many venders invest in lots of money and people on WCDMA cellular systems. What venders consider is the performance of the system. A good call admission control (CAC) scheme can improve the performance and maintain the quality of service (QoS) requirements of the system. To design a suitable CAC scheme for WCDMA cellular systems is important and necessary. In this thesis, we propose a neural fuzzy call admission and rate control (NFCAC-RC) scheme. Considering the outage probabilities of all services, forced termination probability, the interference mean at the next time instant, and the influence of a call request on the adjacent cell, NFCAC-RC guarantee the QoS requirements and maximize the utilization of the system.

In addition, we consider the influences of different data source models in the system. When the system is heavily loaded with bursty data traffics, it is hard to maintain the QoS requirements. NFCAC-RC overcomes this situation by adopting rate control. Simulation results show that NFCAC-RC can improve performance.

誌　謝

首先，我由衷地感謝我的指導教授張仲儒教授在這兩年來給我的指導與教誨，除了在專業研究上的啟發，在做人處事方面也讓我獲益良多。再來我要感謝陳義昇學長給我許多寶貴的建議，沈家慶學長幫我解決程式的問題，以及林立峯學長為我釐清許多觀念。我還要感謝實驗室的學長姊和同學們給予我在課業上及生活上的照應。

兩年的碩士生涯即將畫上句點，在寬頻網路實驗室的這段日子是我人生中珍貴的回憶。最後，我要感謝父母親以及家人給我的幫助與鼓勵，讓我這兩年來可以專心於論文研究。我要將我的碩士論文獻給所有愛護我的人，願你們與我一起分享心中的喜悅。

郭立忠 謹誌

民國九十四年

Contents

List of Figures

List of Tables

Chapter 1

Introduction

Wideband code division multiple access (WCDMA) is used as a radio interface for the third generation (3G) mobile systems. It has been chosen by European Telecommunications Standards Institute (ETSI) as the basic radio access technology for the universal mobile telecommunications system (UMTS). Both Europe and Japan have adopted the WCDMA standard for their third generation wireless services [1], [2]. WCDMA system can reach speeds up to 2 Mbps, which supports higher rate packet data services. The coverage and capacity are significantly improved.

In recent years, WCDMA has been one of the focuses which draw most attention. Many venders invest in lots of money and people on WCDMA cellular systems. What venders consider is the performance of the system. A good call admission control (CAC) scheme can improve the performance and maintain a high utilization of the system. To design a suitable CAC scheme for WCDMA cellular systems is important and necessary.

In WCDMA systems, the uplink load can be regarded as the total interference that the base station (BS) receives [4], [5], and admitting a new call will increase the interference in cellular systems. When the system is heavily loaded and a new call is accepted, the increasing interference may cause the system to enter a state of which the quality-of-service (QoS) requirements of existing calls in the system may not be guaranteed. Notice that this WCDMA system will support multimedia and multirate services. A higher data rate service will cause more interference to the system. Therefore, it is more complicated to design CAC scheme for WCDMA cellular systems providing multirate services to limit the interference.

Number-based CAC and interference-based CAC are two basic methods for call admission control. Interference-based CAC method is more suitable with respect to the interference-limited attribute of WCDMA cellular systems [3]. Shin, Cho, and Sung [4] proposed an interference-based channel assignment scheme for DS-CDMA cellular systems. Instead of a fixed link capacity, the scheme calculates the current interference margin and the handoff interference margin. If the interference after the channel assignment is below the allowed level which is determined by the network, a new channel is assigned to the new call. In [5], Dimitriou and Tafazolli developed a mathematical model to maintain system stability with minimum outage probability. According to the residual capacity of the home and adjacent cells, the system can measure the current level of multiple access interference (MAI) and then decide a new call is accepted or blocked. These schemes used the interference at the present time instant to determine the acceptance of the call request. However, the present interference will change right after the acceptance of a new call. It makes the decision imprecise.

Shen *et al.* [6] proposed an intelligent call admission controller (ICAC) for WCDMA cellular systems to support differentiated quality of service provisioning. In the scheme, fuzzy equivalent interference estimator determines the interference power incurred by the new call request, pipeline recurrent neural network (PRNN) accurately predicts the next-step existing-call interference, and fuzzy call admission processor makes admission decision for the call request. However, ICAC does not consider the leading conditions of adjacent cells. The user position can affect the interference to adjacent cell base stations. Accepting a user near the cell boundary can make the interference experienced by the adjacent cell higher and increase the outage probability, even if the home cell interference is low [7]. If the CAC scheme does not consider the adjacent cells' residual capacity, it does not lead to an optimum resource allocation [5].

Besides, one of the promising important applications of WCDMA systems is the World

Wide Web (WWW) transfers. Wireless data services such as on-line games, music downloads and photo messaging are in wide use. The traditional Poisson traffic model is not suitable for the internet service. The WWW traffic is bursty on many or all time scales. It can be modeled as a self-similar process [8]. The self-similar traffic is obtained as the effect of multiplexing a large number of ON/OFF sources which have heavy-tailed ON and OFF period lengths. ICAC cannot serve such bursty traffic. Most data users will be rejected because ICAC allows the bursty traffic be transmitted without delay. Since data services can tolerate delays, a rate control scheme should be adopted to overcome this situation [9].

Additionally, intelligent techniques such as fuzzy logics, neural networks, and neural fuzzy networks are effective methods to perform radio resource management. In [10], Lo, Chang, and Shung used a neural fuzzy call-admission and rate controller (NFCRC) to decide whether a call request is accepted or not. NFCRC can guarantee the QoS and provide an appropriate rate for users. Instead of the rate control in [11] that the transmission rate is adaptively modified from one time slot to another, the rate control in [10] allocates the transmission rate for the user until the connection is finished. The method in [10] is a good choice for its simplicity, but it is not suitable to transmit a fixed rate during the hole connection time. The variation of the transmitting situation should be considered. It is more suitable to allocate a fixed rate at the beginning of the burst-mode traffic.

The paper proposes a neural fuzzy call admission control method for WCDMA cellular systems supporting multirate services. It contains a PRNN/ERLS interference predictor to predict the next time instant existing-call interference, and a neural fuzzy call admission and rate controller to determine whether the call request is accepted or not and the transmission rate assigned at the beginning of each data burst. An extended recursive least squares (ERLS) training algorithm for the PRNN has been shown to achieve significantly higher prediction precision values [12]. By using PRNN/ERLS interference predictor, the next time instant existing-call interference can be predicted accurately. The neural network can make the fuzzy

logic systems more adaptive and effective. Adaptive network based fuzzy inference system (ANFIS) [13] is a good choice to fine-tune the membership functions of the fuzzy logic systems. ANFIS is used in this thesis to tune the membership functions of neural fuzzy call admission control.

Considering the adjacent cell interference, our proposed CAC scheme will monitor the adjacent cells' residual capacity by the radio network controller (RNC) and make proper admission decision, which can avoid the outage condition of adjacent cell. The next time instant existing-call interference is used to avoid the outage condition of home cell. According to the QoS measures such as the outage probabilities of all service types and the forced termination probability, the CAC scheme can maintain the QoS requirements. The data source models, which include batch Poisson process and Pareto distributed, are taken into account in the systems, individually. And, in order to increase the system capacity and maintain the QoS requirements, the rate controller is used to determine the transmission rate assigned at the beginning of each data burst.

The performance evaluation will be based on the QoS requirements and the utilities of the system. Instead of the considerations in [14] that the new-call-blocking probability and the handoff-dropping probability are measured, only handoff dropping probability is adopted in the performance measurement. New-call-blocking probability is not considered because the system utilities should be focus on the mean number of users and packets per second transmitted in a cell.

The rest of the thesis is organized as follows. Chapter 2 describes the system model of a WCDMA cellular system. Chapter 3 gives the designs for the PRNN/ERLS interference predictor, and the neural fuzzy call admission and rate controller. Two scenarios are illustrated in chapter 4, and the simulation results and discussions are presented. Finally, concluding remarks are given in chapter 5.

Chapter 2

System Model

We consider a WCDMA cellular system with K cells and a large number of wireless users. Mobile users communicate with each other via air interface to BS, and BSs are connected to a RNC. The WCDMA cellular system has different frequency bands for the uplink and the downlink. Each base station has an omni antenna located at center in the cell. A user arriving at the system will choose its home cell of which the radio propagation attenuation is the smallest. Mobility of users is modeled and users are assumed to be uniformly distributed within each cell. The number of pseudo-noise (PN) codes available for code-division multiplexing is assumed to be large enough to support all services. Only the first-tier adjacent cells' interference is considered.

2.1 Propagation Model

In the radio propagation, two main factors are considered which are the path loss and the shadowing effects. Compensated by perfect power control scheme, the effect of short-term fading is ignored. The propagation loss is generally modeled as the product of the q th power of the distance and a log-normal component representing shadowing losses. Thus, the radio propagation (link gain) model, $L(r)$, is given by

$$L(r) = 10^{\frac{z}{10}} r^{-q}, \qquad (2.1)$$

where r is the distance between the mobile user and the base station. z is the decibel attenuation due to shadowing, with zero mean and standard deviation s . q is the path loss exponent.

2.2 Source Model

Input traffic generated within mobile users is classified into two types of service as real-time voice (type-1) and non-real-time data (type-2). New voice and data calls arrive at the system according to Poisson distributions with average arrival rates of l_v and l_d, respectively. Every voice source is characterized by a two-state (ON and OFF) discrete-time Markov chain traffic model and will generate one air-interface packet in each frame time of T during ON state (talk spurts) but none during OFF state (silence). The mean durations of talk spurts and silence periods are assumed to be exponentially distributed with $1/a$ and $1/b$, respectively. The ON/OFF source model is shown in Fig. 2.1 as described in [15]. All air-interface packets generated in a talk spurts form a voice message.

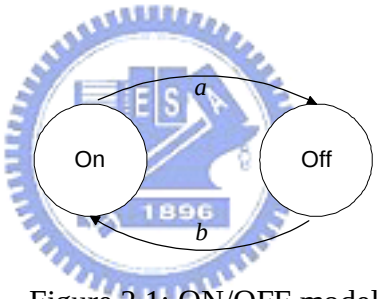

Figure 2.1: ON/OFF model

On the other hand, the data source is characterized by a batch Poisson process with an average message arrival rate A_d. The size of data message is assumed to be a positive-valued random variable, which is generally distributed. The data message will further be segmented into a number of air-interface packets according to the processing gain set for the service.

If the bursty traffic condition is considered, the data source is characterized by a self-similar process and the packets are Pareto distributed, as shown in [11]. When a data session arrives to the system, it is consisted of a number of packet call requests, N_{pc}, which is geometrically distributed with mean $m_{N_{pc}}$ as described in [16],[17]. The packet call

requests are separated by reading time, D_{pc}, which is geometrically distributed with mean $m_{D_{pc}}$. Each packet call consists of a number of packets, N_p, which is geometrically distributed with mean m_{N_p}. The time interval between two consecutive packets, D_p, is geometrically distributed with mean m_{D_p}. The packet size, S_p, is modeled as a Pareto distribution. The Pareto distribution is defined by:

$$f_x(x) = \frac{a_p \cdot k_p^{a_p}}{x^{a_p+1}}, \quad x \geq k_p \tag{2.2}$$

$$F_x(x) = 1 - \left(\frac{k_p}{x}\right)^{a_p}, \quad x \geq k_p \tag{2.3}$$

$$m = \frac{k_p a_p}{a_p - 1}, \quad a_p > 1 \tag{2.4}$$

$$s^2 = \frac{k_p^2 \cdot a_p}{(a_p - 2) \cdot (a_p - 1)^2}, \quad a_p > 2 \tag{2.5}$$

where a_p is the Pareto distribution parameter and k_p is the minimal packet size (bytes). The packet size is defined as the following formula:

$$S_p = \min(P, m) \tag{2.6}$$

where P is normal Pareto distributed random variable ($a_p = 1.1$, $k_p = 81.5$ bytes) and m is maximum allowed packet size, $m = 66666$ bytes. The data session is depicted in Fig. 2.2.

Each terminal supports two finite separate buffers for voice and data services. Also, the distributions of the holding times for voice and data call were assumed to be exponentially distributed. Voice and data terminals in a cell transmit their packets by sharing the common air interface. When a packet in a terminal is ready for transmission, the transmitter waits until the beginning of the next slot and begins transmitting. For multirate services, we pair up multiple basic channels until the required data rate is achieved.

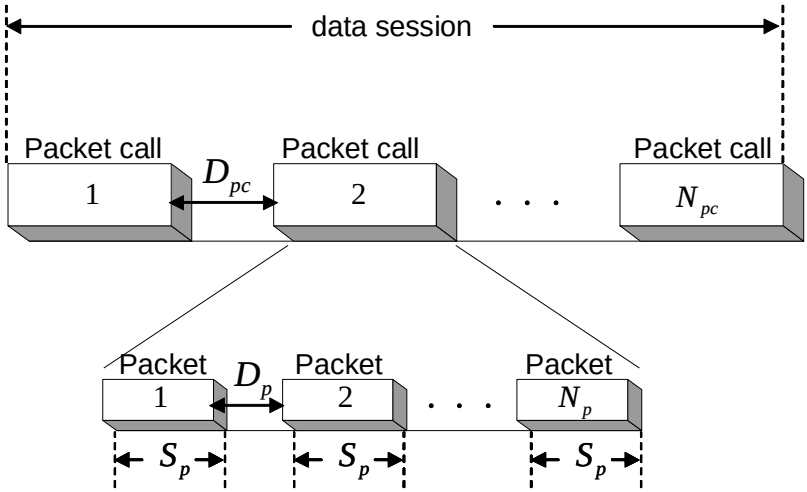

Figure 2.2: Data session

2.3 Interference Model

For differentiated bit-error-rate (BER) requirements set for the type-1 and type-2 traffic, we define their individual processing gains, which are denoted by G_1 and G_2. The G_1 and G_2 are chosen to be the closest integer greater than the required spreading factor. Corresponding to each specific BER requirement and processing gain, the signal-to-interference ratio (SIR) threshold values of type-1 and type-2 traffic, denoted by SIR_1^* and SIR_2^*, can be obtained. Two basic transmission rates (basic channels) are supported: 1) $R_1 = R$, which is dedicated to active voice users and is equal to the voice coding rate and 2) $R_2 = R \cdot G_1 / G_2$, which is dedicated to active data users. If a data user requires a transmission rate X higher than the basic transmission rate R_2, this rate will be quantized into M times of R_2, where $M = \lceil X / R_2 \rceil$ and $\lceil \cdot \rceil$ denotes the smallest integer greater than or equal to the argument. Each R_2 is encoded with a different pseudo-noise code.

All users in their home cell are assumed to be perfectly power controlled, and the power

level of basic channel received at the base station is a constant value S. During the connection, as the user detects the pilot strength of adjacent cell stronger than that of home cell by j dB, the handoff procedure is performed. Assume that there are $N_{1,k}$ type-1 users and $N_{2,k}$ type-2 users in home cell k for communication. n_i denotes the type-1 traffic activity factor and d_i denotes the type-2 traffic activity factor. The home cell interference, $I_{H,k}(n)$, can be obtained by

$$I_{H,k}(n) = S\left[\sum_{i=1}^{N_{1,k}} n_i + \sum_{i=1}^{N_{2,k}} d_i \cdot R_G \cdot M_{i,k}(n)\right], \tag{2.7}$$

where $M_{i,k}(n)$ is a random variable, denoting that the number of basic code channels needed by type-2 user i in home cell k for communication, and $R_G = R_2/R_1$. And the first-tier adjacent cell interference, $I_{A,k}(n)$, is given by

$$I_{A,k}(n) = S\sum_b \left[\sum_{i=1}^{N_{1,b}} n_i \cdot \left(\frac{r_{ib}}{r_{ik}}\right)^q \cdot 10^{\frac{z_{ik}-z_{ib}}{10}} + \sum_{i=1}^{N_{2,b}} d_i \cdot R_G \cdot M_{i,b}(n) \cdot \left(\frac{r_{ib}}{r_{ik}}\right)^q \cdot 10^{\frac{z_{ik}-z_{ib}}{10}}\right], \tag{2.8}$$

where $b \in$ {the first-tier adjacent cells neighboring to cell k}, r_{ik} is the distance of the user i in cell b to the base station of cell k, and r_{ib} is the distance of the user i in cell b to the base station of its home cell. Therefore, the interference power of cell k at time instant n, which is denoted by $I_k(n)$, is the summation of $I_{H,k}(n)$ and $I_{A,k}(n)$.

Chapter 3

Neural Fuzzy Call Admission and Rate Controller

In this chapter, the system parameters are introduced first. Then the PRNN/ERLS interference predictor is described. Finally, the design of neural fuzzy call admission and rate controller is presented.

3.1 System Parameters

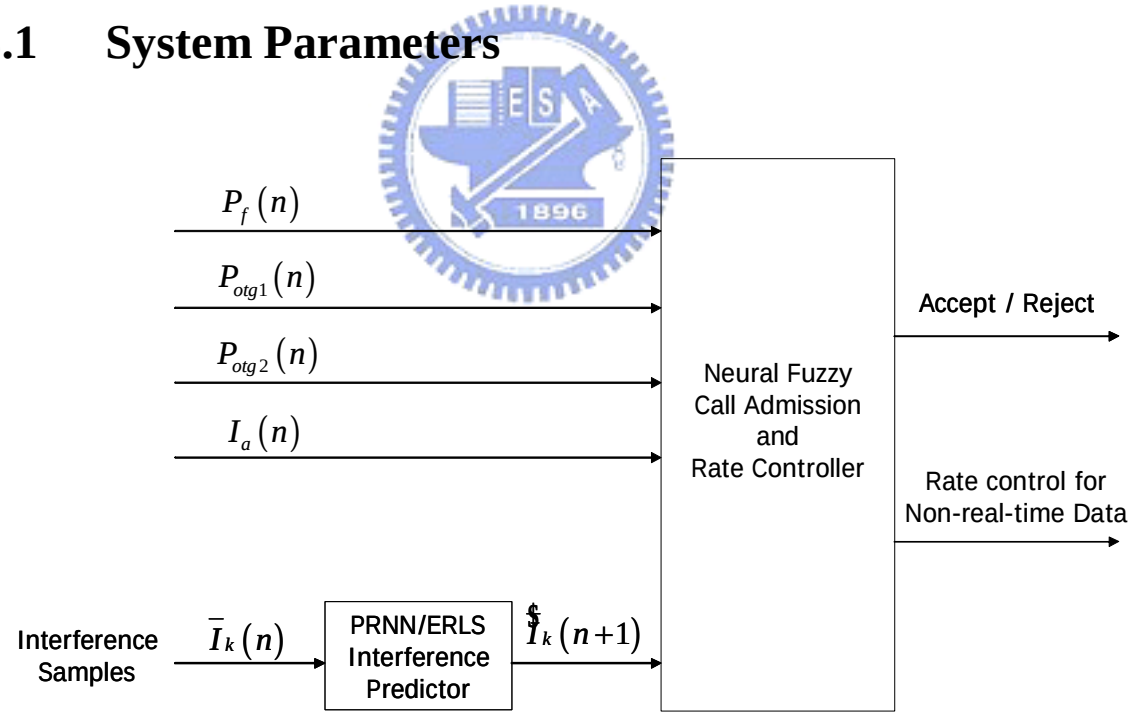

Figure 3.1: System architecture

Fig. 3.1 depicts the system architecture of the proposed neural fuzzy call admission and rate controller. Notably, the *rate controller* only works for non-real-time data user.

The proposed CAC consists of a *PRNN/ERLS interference predictor*, and *neural fuzzy call admission and rate controller*. The *PRNN/ERLS interference predictor* takes the interference mean of cell k at the present time instant n, $\bar{I}_k(n)$, as an input variable to accurately predict the interference mean at the next time instant $(n+1)$, $\hat{I}_k(n+1)$. The $\bar{I}_k(n)$ is obtained by

$$\bar{I}_k(n) = \frac{\sum_{j=0}^{N-1} I_k(n-jT)}{N}, \tag{3.1}$$

where N is the size of time window, and $I_k(q)$ is the received interference power at time instant q. And the *neural fuzzy call admission and rate controller* chooses the forced termination probability for handoffs measured at present time n, denoted by $P_f(n)$, the outage probabilities of type-1 and type-2 services measured at the present time n, denoted by $P_{otg1}(n)$ and $P_{otg2}(n)$, the influence of a call request on the adjacent cell base stations, denoted by $I_a(n)$, and $\hat{I}_k(n+1)$ as input variables to determine the acceptance for the call request. If the call request is a non-real-time data, the *neural fuzzy call admission and rate controller* allocates an appropriate rate for the user. The influence of a call request on the adjacent cell base stations, I_a, is given by

$$I_a(n) = \underset{\forall b \in \{adjacent\ cell\}}{Max} \left\{ \bar{I}_{a_b}(n) \middle| L_{a_b} > L_{th} \right\}, \tag{3.2}$$

where $\bar{I}_{a_b}(n)$ is the interference mean of adjacent cell b at the present time instant n, L_{a_b} is the link gain from the call request to the base station of adjacent cell b, and L_{th} is the threshold that the call request can cause significant influence to the adjacent cell base station. In a hexagonal cellular system, a user at cell boundary can influence at most three cells. So, there are at most two adjacent cells in the equation (3.2).

Voice service requires less bandwidth but no delays. On the other hand, data service can tolerate moderate delays and permit a variable rate transmission scheme. For data source, the rate control scheme will assign the transmission rate at the beginning of each packet burst.

According to $\hat{I}_k(n+1)$ and $I_a(n)$, a proper transmission rate is allocated to the packet burst. Mobile user will obey the assignment from home base station and transmits the packet. If the packet cannot be transmitted in one frame time, the remained bits of the packet will be transmitted at next frame time obeying the assigned transmission rate until all of the bits are transmitted. To storage the packets waiting for transmitting, the buffer for data service must be large enough.

In the paper, the required outage probability for type-i traffic, denoted by P_{otgi}^*, is set to be the system QoS requirements. In order to protect the handoff connection against forced termination, the required forced termination probability, denoted by P_f^*, is also set to be the QoS requirement.

3.2 PRNN/ERLS Interference Predictor

In the WCDMA cellular systems, the interference measured at the base station is non-linear and non-stationary. Instead of using the traditional auto-regressive moving average (ARMA) model, the interference process is assumed to be in a nonlinear ARMA (NARMA) model due to its non-linearity. Approximating the NARMA model, with one-step prediction, we can express the mean interference as a function of p measured interference powers and q previously predicted interference powers. That is,

$$\hat{I}_k(n+1) = H\left(\bar{I}_k(n), \mathbf{K}, \bar{I}_k(n-p+1); \hat{I}_k(n), \mathbf{K}, \hat{I}_k(n-q+1)\right), \qquad (3.3)$$

where $\hat{I}_k(i)$ is the previously predicted mean interference sample at time i, $n-p+1 \le i \le n$, and $H(\cdot)$ is an unknown nonlinear function to be determined.

Since the neural network prediction is a fast, low complexity, and non-linear one that can estimate the non-linear and time-varying value of WCDMA interference, we adopt PRNN to approximate the function $H(\cdot)$. PRNN prediction yields a high prediction accuracy, fast convergent speed, and low computation complexity. It is a good choice for us

to predict the next time system existing calls' mean interference.

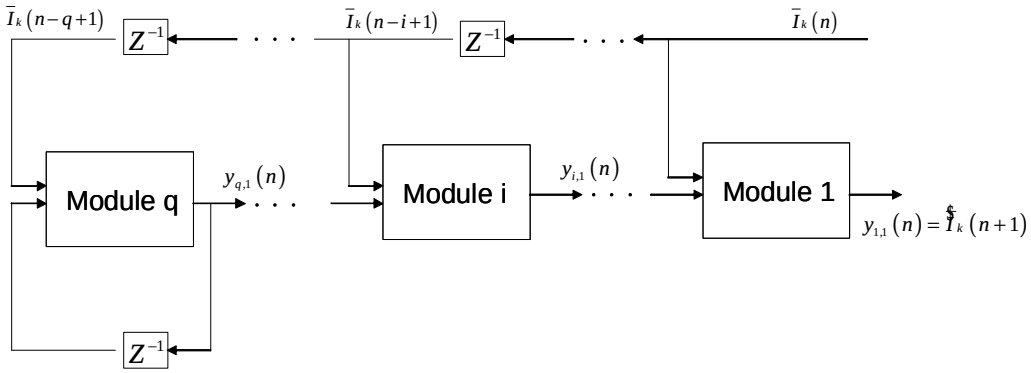

Figure 3.2: Structure of the PRNN interference predictor

Fig. 3.2 shows the architecture of PRNN interference predictor, which involves a total of q levels of processing. Each level has an identical neural module and a subtractor. For level i, two external inputs are fed into the module: the delayed version of the measured interference sample $\bar{I}_k(n-i+1)$ and the first output of the preceding level $y_{i+1,1}(n)$, and the output of this module subtracted from $\bar{I}_k(n-i+2)$ forms an error signal $e_i(n)$. The error signal is used to adjust the synaptic weights in the ith neural module. Consequently, the output of the first module $y_{1,1}(n)$ is the desired next-step interference prediction $\hat{\bar{I}}_k(n+1)$.

Fig. 3.3 depicts the detailed structure of module i, which is constituted by a two-layer recurrent neural network (RNN). Each module is constituted of a neural network part and a comparator. The output vector, $\vec{y}_i(n)=[y_{i,1}(n),\mathbf{K},y_{i,M}(n)]$, consists of M elements, among which, $(M-1)$ outputs are fed back to the input, and the first output, $y_{i,1}(n)$, is applied directly to the next module $i-1$. The input vector $\vec{u}_i(n)$ consists of three parts: the p-tuple external input vector $[\bar{I}_k(n-i+1),\ \mathbf{K},\bar{I}_k(n-i-p+2)]$, a bias input whose value is always maintained at $+1$, a feedforward input from the preceding level $y_{i+1,1}(n)$, and the M-tuple feedback vector $\left[y_{i,2}(n-1),\mathbf{K},y_{i,M}(n-1)\right]$. The dimension of the prediction

order p is a design parameter such that the PRNN can approximate the NARMA process more accurate and efficient. The input vector can be defined by

$$\vec{u}_i(n) = \left[\bar{I}_k(n-i+1), \mathbf{L}, \bar{I}_k(n-i-p+2), 1, \right.$$
$$\left. y_{i+1,1}(n), y_{i,2}(n-1), \mathbf{L}, y_{i,M}(n-1)\right]. \qquad (3.4)$$

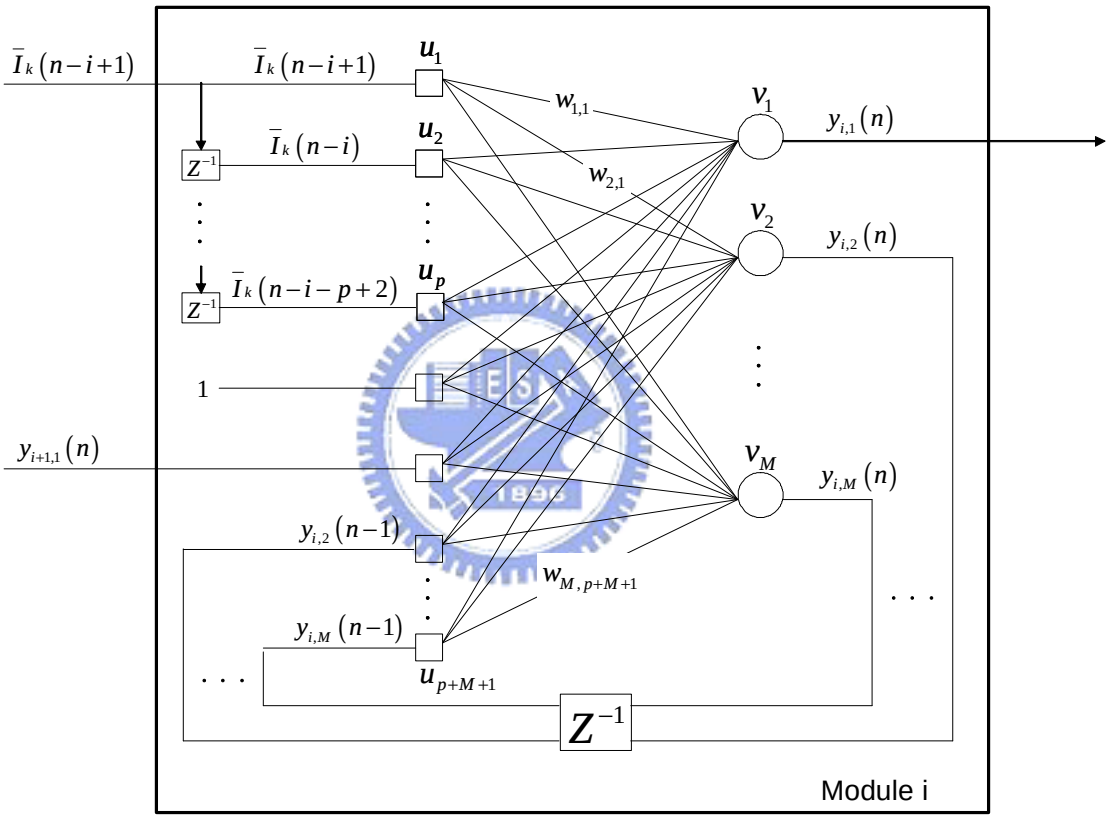

Figure 3.3: The i th small RNN module in the PRNN interference predictor

The $p+M+1$ neurons of input layer are fully connected to M neurons of output layer by a M -by- $(p+M+1)$ synaptic weight matrix W. An element $w_{k,j}$ of W represents the weight of the connection from the j th input node to the k th output node. Let $v_{i,k}(n)$ to be the net input of the k th neuron at output layer, thus, $\vec{v}_i(n)$ will be

$$\mathbf{v}_i(n) = W\mathbf{u}_i(n). \tag{3.5}$$

And $v_{i,k}(n)$ is defined by

$$\begin{aligned} v_{i,k}(n) = & \sum_{j=1}^{p} w_{k,j}\bar{I}_k\left(n-(i+j-2)\right) + w_{k,(p+1)} \\ & + w_{k,(p+2)}y_{i+1,1}(n) + \sum_{j=p+3}^{p+M+1} w_{k,j}y_{i,(j-p-1)}(n-1). \end{aligned} \tag{3.6}$$

The activation function of each neuron $f(\cdot)$ is a sigmoid function described by logistic function

$$y_{i,k}(n) = f\left(v_{i,k}(n)\right) = \frac{1}{1+\exp\left(-v_{i,k}(n)\right)}, \tag{3.7}$$

where $i = 1, \mathbf{L}, q$, and $k = 1, \mathbf{L}, M$.

The first output signal $y_{i,1}(n)$ of each module is also fed into a comparator. Each comparator subtract $\bar{I}_k(n-i+2)$ from $y_{i,1}(n)$ to form an error signal $e_i(n)$, which is defined as

$$e_i(n) = \bar{I}_k(n-i+2) - y_{i,1}(n). \tag{3.8}$$

Because $y_{i,1}(n)$ is limited in amplitude within the range (0,1) due to the characteristics of sigmoid activation function, $\bar{I}_k(n-i+2)$ is normalized before being actually put into the PRNN predictor.

The prediction error can be used for updating the weights. Here, the extended recursive least square (ERLS) is applied as the learning algorithm for PRNN [18]. The prediction errors of all modules in the PRNN are combined as

$$E(n) = \sum_{i=1}^{q} l^{i-1}e_i^2(n), \tag{3.9}$$

where $l \in (0,1]$ is the forgetting factor. The term l^{i-1} is an approximate measure of the memory of the individual modules in the PRNN. The cost function of ERLS is defined as

$$e_{ERLS}(n) = \sum_{k=1}^{n} l^{n-k}E(k). \tag{3.10}$$

The ERLS algorithm minimizes the cost function, equation (3.10), and then updates the

weights of the neurons in the modules accordingly.

The training of PRNN/ERLS consists of two stages. During the off-line training phase, interference samples using typical system parameters and traffic load are generated. The PRNN/ERLS, fed with these samples, adjusts the synaptic weights recursively until the root mean square error (RMSE) of the desired prediction output is lower than the criteria. During the on-line training phase, the PRNN interference predictor obtains the interference predictions for existing calls at time instant (n+1), $\hat{I}_k(n+1)$, from the output of the first neuron of the first module, and measures the interference sample $\bar{I}_k(n+1)$; then it adjusts the synaptic weights using the ERLS algorithm. Due to the on-line learning capability, PRNN/ERLS can adapt its weights to the current load conditions. So, PRNN/ERLS is appropriate for being applied to interference prediction in WCDMA system.

3.3 Design of Neural Fuzzy Call Admission and Rate Controller

A neural fuzzy controller is an integration of the fuzzy logic system and the neural network. The integration brings the low-level learning and computation power of the neural network into the fuzzy logic system, and provides the high-level, humanlike thinking and reasoning of fuzzy logic system into the neural network.

3.3.1 Fuzzy Logic Controller

A fuzzy set F in an universe of discourse U is characterized by a membership function which takes values in the interval $(0,1)$. A linguistic variable x in U is defined by $T(x)=\{T_x^1, T_x^2, \mathbf{L}, T_x^k\}$ and $M(x)=\{M_x^1, M_x^2, \mathbf{L}, M_x^k\}$, where $T(x)$ is a term set of x, i.e., a set of terms T_x^i with membership function M_x^i defined on U, and $M(x)$ is a semantic rule for associating each term with its meaning.

A fuzzy logic controller has functional blocks of a fuzzifier, a defuzzifier, and an inference engine containing a fuzzy rule base, as shown in Fig. 3.4. The fuzzifier is a mapping from observed m-dim inputs x_i to fuzzy set $T_{x_i}^{k_i}$ with degree $M_{x_i}^{k_i}$, $i = 1, \mathbf{L}, m$. The fuzzy rule base is a control knowledge-base characterized by a set of linguistic statements in the form of "if-then" rules that describe a fuzzy logic relationship between m-dim inputs x_i and n-dim outputs z_j. The inference engine is a decision-making logic that acquires the input linguistic terms of $T(x_i)$ from the fuzzifier and uses a inference method to obtain the output linguistic terms of $T(z_j)$. The defuzzifier adopts a defuzzification function to convert $T(z_j)$ into a non-fuzzy value that represents decision z_j.

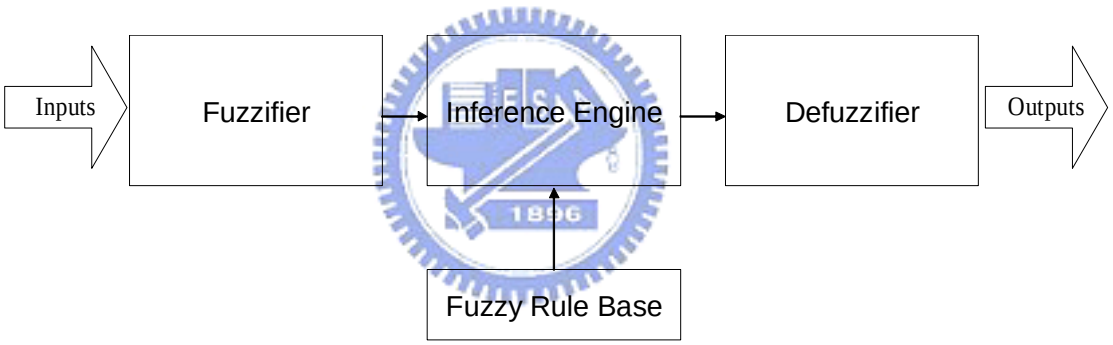

Figure 3.4: Fuzzy system

3.3.2 Neural Network

A multi-layer feedforward neural network is a layered network which consists of an input layer, an output layer, and at least one hidden layer. The hidden layer consists of nonlinear processing elements, called nodes. Nodes between two adjacent layers are fully interconnected with variable link weights. The output of a node in one layer multiplied by the link weight becomes the input of a node in the next layer. Each node forms a weighted sum of its inputs and generates an output according to a predefined activation functions $a(\cdot)$.

Consider a feedforward network $NN(X,W)$ with input vector X and a set of weight vector W which will be updated by some learning rules. It is desired to train $NN(X,W)$ (actual output) to approximate a desired output function $z(X)$ as close as possible.

3.3.3 Neural Fuzzy Controller

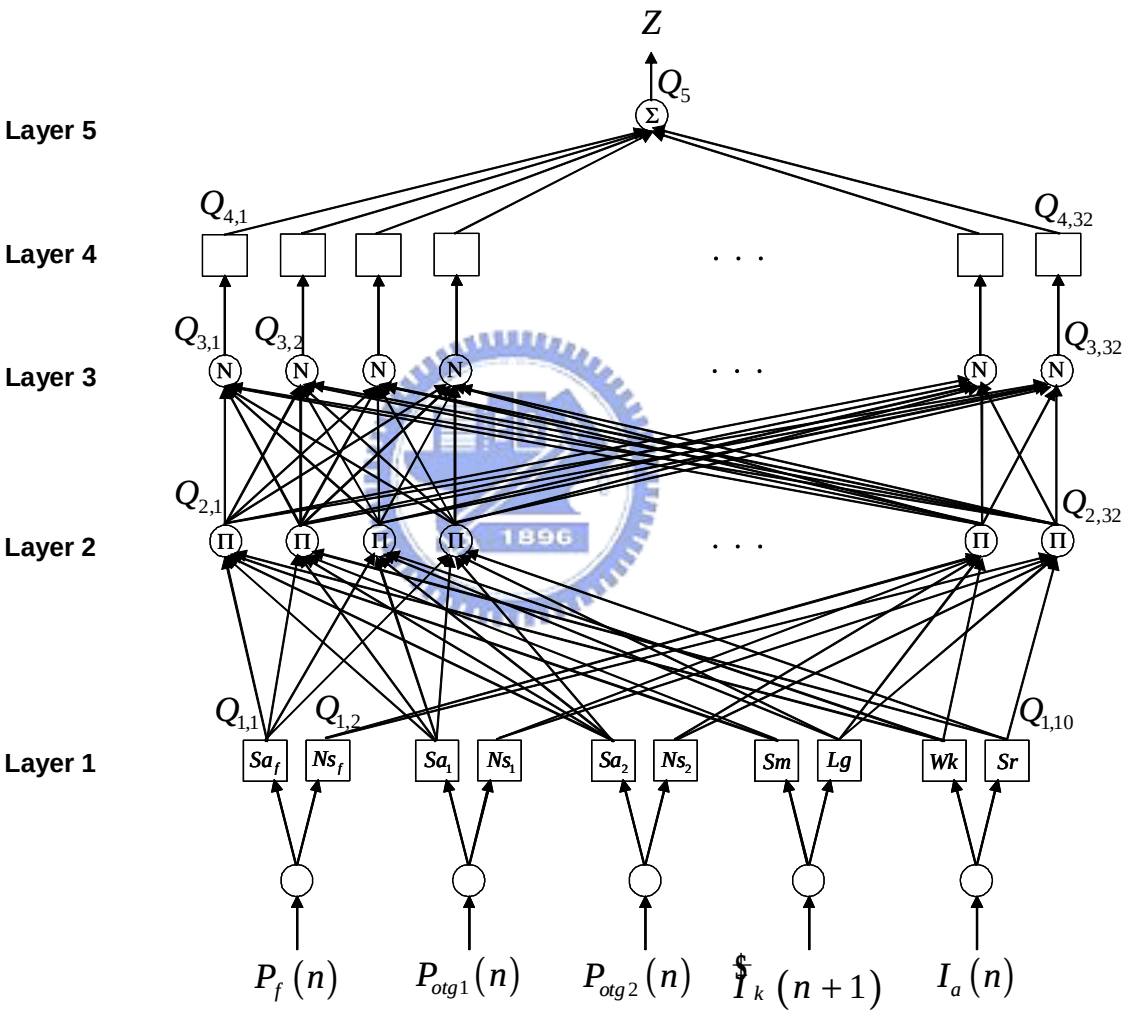

Figure 3.5: The structure of the neural fuzzy call admission and rate controller

We adopt a five-layer neural fuzzy controller which is implemented by ANFIS to design the neural fuzzy call admission and rate controller. The adaptive-network-based fuzzy inference system (ANFIS) employs the adaptive network architecture to represent the fuzzy

inference system. ANFIS can be applied to a wide range of areas, such as nonlinear function modeling, time series prediction, and fuzzy controller design [19], [20].

The fuzzy inference system under consideration has five linguistic variables ($P_f(n)$, $P_{otg1}(n)$, $P_{otg2}(n)$, $\hat{I}_k(n+1)$, and $I_a(n)$) and each variable is divided into two fuzzy terms. Fig. 3.5 shows the corresponding equivalent ANFIS architecture, which represents the first-order Sugeno fuzzy model. The node functions of each layer are similar and they are described as below:

Layer 1: Every node i in this layer is an adaptive node with a node function

$$Q_{1,i} = \begin{cases} m_{Sa_f}\left(P_f(n)\right), & for\ i=1 \\ m_{Ns_f}\left(P_f(n)\right), & for\ i=2 \\ \quad \mathbb{M} \\ m_{Sr}\left(I_a(n)\right), & for\ i=10 \end{cases}, \tag{3.11}$$

where $P_f(n)$ ($P_{otg1}(n)$, $P_{otg2}(n)$, $\hat{I}_k(n+1)$, or $I_a(n)$) is the input to the node i and Sa_f (Ns_f, Sa_1, Ns_1, Sa_2, Ns_2, Sm, Lg, Wk or Sr) is a linguistic term associated with this node. $m_{Sa_f}, \mathbf{L}, m_{Sr}$ is the membership function for the term $Sa_f, \mathbf{L}, Sr$. Each node function specifies the degree to which the given input $P_f(n)$ ($P_{otg1}(n)$, $P_{otg2}(n)$, $\hat{I}_k(n+1)$, or $I_a(n)$) satisfies the qualifier Sa_f (Ns_f, Sa_1, Ns_1, Sa_2, Ns_2, Sm, Lg, Wk or Sr).

Layer 2: Every node i in this layer is a fixed node labeled Π. The output of node i, denoted by $Q_{2,i}$, is the product of all the incoming signals for the i-th rule. It is given by

$$Q_{2,i} = w_i = \begin{cases} m_{Sa_f}\left(P_f(n)\right)\times m_{Sa_1}\left(P_{otg1}(n)\right)\times m_{Sa_2}\left(P_{otg2}(n)\right)\times m_{Sm}\left(\hat{I}_k(n+1)\right)\times m_{Wk}\left(I_a(n)\right), & for\ i=1 \\ m_{Sa_f}\left(P_f(n)\right)\times m_{Sa_1}\left(P_{otg1}(n)\right)\times m_{Sa_2}\left(P_{otg2}(n)\right)\times m_{Sm}\left(\hat{I}_k(n+1)\right)\times m_{Sr}\left(I_a(n)\right), & for\ i=2 \\ \quad \mathbb{M} \\ m_{Ns_f}\left(P_f(n)\right)\times m_{Ns_1}\left(P_{otg1}(n)\right)\times m_{Ns_2}\left(P_{otg2}(n)\right)\times m_{Lg}\left(\hat{I}_k(n+1)\right)\times m_{Sr}\left(I_a(n)\right), & for\ i=32 \end{cases}. \tag{3.12}$$

Each node output represents the firing strength of i-th rule and performs the fuzzy AND operation.

Layer 3: Every node i in this layer is a fixed node labeled N. The i-th node calculates the ratio of the i-th rule's firing strength to the sum of all rules' firing strengths. The output of node i, denoted by $Q_{3,i}$, is called normalized firing strength and calculated as

$$Q_{3,i} = \overline{w}_i = \frac{w_i}{\sum_{j=1}^{32} w_j}. \tag{3.13}$$

Layer 4: Every node i in this layer is an adaptive node with a node function

$$Q_{4,i} = \overline{w}_i \times f_i = \overline{w}_i \times (p_i \times X + q_i \times Y + r_i), \quad 1 \le i \le 32 \quad , \tag{3.14}$$

where $Q_{4,i}$ is the output, f_i is a crisp output in the consequent, and p_i, q_i, r_i are the consequent parameter sets of node i.

Layer 5: The single node in this layer is a fixed node labeled Σ, which computes the overall output Q_5 as the summation of all incoming signals.

$$Q_5 = \sum_{i=1}^{32} Q_{4,i} = \sum_{i=1}^{32} \overline{w}_i f_i = \frac{\sum_{i=1}^{32} w_i f_i}{\sum_{j=1}^{32} w_j} \tag{3.15}$$

For the new call request, the processor considers the $P_f(n)$, $P_{otg1}(n)$, $P_{otg2}(n)$, $I_a(n)$, and $\hat{I}_k(n+1)$ as its input linguistic variables which indicate the system performance measures, the influence of the call request on the adjacent cell base stations, and the predicted system load. For the handoff call request, the processor considers the same input variables as for the new call request except $I_a(n)$ since the influence of a handoff call on the adjacent cell base stations has already in the system. The adjacent cells have already considered this influence as $I_a(n)$ is included in its interference. For the rate control, the processor considers $I_a(n)$, and $\hat{I}_k(n+1)$ as its input linguistic variables. These two parameters indicate the system loading. The assigned transmission rate for data user will be reduced if the system loading is high.

The details of *Layer 1* are described as follows. According to the domain knowledge from simulations, term sets and membership functions of input linguistic variables $P_f(n)$,

$P_{otg1}(n)$, $P_{otg2}(n)$, $I_a(n)$, and $\hat{I}_k(n+1)$ are defined in Table 3.1, in which trapezoidal function $h(x;x_0,x_1,a_0,a_1)$ is chosen to be the membership function and is given by

$$h(x;x_0,x_1,a_0,a_1)=\begin{cases}\dfrac{x-x_0}{a_0}+1 & for \quad x_0-a_0<x\le x_0\\ 1 & for \quad x_0<x\le x_0\\ \dfrac{x_1-x}{a_1}+1 & for \quad x_1<x\le x_1+a_1\\ 0 & otherwise\end{cases}, \tag{3.16}$$

where, as shown in Fig. 3.6, x_0 (x_1) in $h(\cdot)$ is the left (right) edge of the trapezoidal function, and a_0 (a_1) is the left (right) width of the trapezoidal function.

	Elements of term sets	Membership function
$P_f(n)$	Satisfied (Sa_f)	$m_{Sa_f}(P_f(n))=h(P_f(n);0,Sa_{e_f},0,Sa_{w_f})$
	Not satisfied (Ns_f)	$m_{Ns_f}(P_f(n))=h(P_f(n);Ns_{e_f},1,Ns_{w_f},0)$
$P_{otg1}(n)$	Satisfied (Sa_1)	$m_{Sa_1}(P_{otg1}(n))=h(P_{otg1}(n);0,Sa_{e1},0,Sa_{w1})$
	Not satisfied (Ns_1)	$m_{Ns_1}(P_{otg1}(n))=h(P_{otg1}(n);Ns_{e1},1,Ns_{w1},0)$
$P_{otg2}(n)$	Satisfied (Sa_2)	$m_{Sa_2}(P_{otg2}(n))=h(P_{otg2}(n);0,Sa_{e2},0,Sa_{w2})$
	Not satisfied (Ns_2)	$m_{Ns_2}(P_{otg2}(n))=h(P_{otg2}(n);Ns_{e2},1,Ns_{w2},0)$
$\hat{I}_k(n+1)$	Small(Sm)	$m_{Sm}(\hat{I}_k(n+1))=h(\hat{I}_k(n+1);0,Sm_e,0,Sm_w)$
	Large(Lg)	$m_{Lg}(\hat{I}_k(n+1))=h(\hat{I}_k(n+1);I_o,\infty,Lg_w,0)$
$I_a(n)$	Weak(Wk)	$m_{Wk}(I_a)=h(I_a;0,Wk_e,0,Wk_w)$
	Strong(Sr)	$m_{Sr}(I_a)=h(I_a;I_o,\infty,Sr_w,0)$

Table 3.1: The term sets and their membership function for input variables

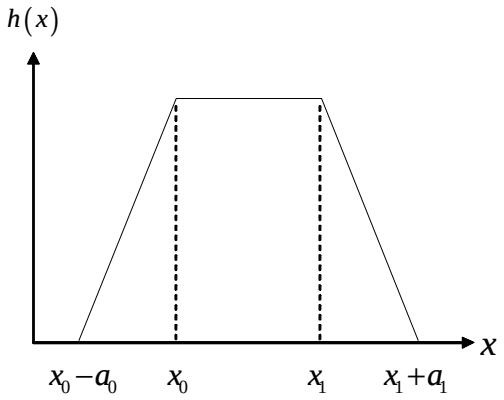

Figure 3.6: The figure of $h(\cdot)$

As for the parameter setting for these membership functions, Ns_{e_f} is set to be P_f^* minus a safety margin, and Sa_{e_f} is a value less than Ns_{e_f} by a safety amount for separating the satisfactory region and the violation region; Ns_{e1} (Ns_{e2}) is set to be P_{otg1}^* (P_{otg2}^*) minus a safety margin, and Sa_{e1} (Sa_{e2}) is also set to a value less than Ns_{e1} (Ns_{e2}) for the same reason as the safety amount for Sa_{e_f} ; I_o is the tolerable interference power corresponding to the minimal signal-to-interference power ratio SIR_1^* . Sm_e and Wk_e would be sets to be fraction of I_o . We also set $Sm_w = I_o - Sm_e = Lg_w$, $Wk_w = I_o - Wk_e = Sr_w$ to simplify the design of fuzzy logic parameters. The other endpoints of Sa_{w_f} , Ns_{w_f} , Sa_{w1} , Ns_{w1} , Sa_{w2} , and Ns_{w2} must be fine-tuned to proper values during simulations. We use ANFIS to tune all of these membership functions.

The fuzzy rules in *Layer 2* are described as follows. According to the fuzzy set theory, the fuzzy rule base of new call forms a fuzzy set with dimensions $\left|T\left(P_f(n)\right)\right|$ Í $\left|T\left(P_{otg1}(n)\right)\right|$ Í $\left|T\left(P_{otg2}(n)\right)\right|$ Í $\left|T\left(\hat{I}_k(n+1)\right)\right|$ Í $\left|T\left(I_a(n)\right)\right|$ ($\left|T(x)\right|$ denotes the number of terms in $T(x)$). Therefore, there are a total of 32 fuzzy inference rules. Table 3.2 and 3.3 list these fuzzy inference rules of new voice call and new data call. The more (less) satisfied the $P_f(n)$, $P_{otg1}(n)$, $P_{otg2}(n)$ are and the smaller (larger) the $\hat{I}_k(n+1)$ is, the higher (lower) likelihood the system can accept the new call request. At any specific system load condition,

the system will tend to reject the bad users with larger influence on the adjacent cell base stations according to $I_a(n)$. Similarly, there are a total of 16 fuzzy inference rules for handoff call request. Table 3.4 and 3.5 list these fuzzy inference rules of handoff voice call and handoff data call. Since dropping an ongoing call is assumed to be more annoying than blocking a new call, it is needed to give a high priority to the handoff calls as compared to new calls. The system tends to accept the handoff call as the $P_f(n)$ is not satisfied more likely than as $P_f(n)$ is satisfied to protect the ongoing call anyway except the condition that the traffic load is very heavy. And the larger $P_{otg1}(n)$, $P_{otg2}(n)$ and $\$I_k(n+1)$ imply the heavier traffic load, then the system tends to reject the handoff call request. For rate controller, there are a total of four inference rules. The smaller $\$I_k(n+1)$ and $I_a(n)$ imply the lighter traffic load, then the system tends to assign a higher transmission rate to the data call. Otherwise, a lower transmission rate will be assigned. Table 3.6 lists these fuzzy inference rules.

Rule	P_f	P_{otg1}	P_{otg2}	$\$I_{n+1}$	I_a	Z_{nv}	Rule	P_f	P_{otg1}	P_{otg2}	$\$I_{n+1}$	I_a	Z_{nv}
1	Sa_f	Sa_1	Sa_2	Sm	Wk	SA_{nv}	17	Ns_f	Sa_1	Sa_2	Sm	Wk	SA_{nv}
2	Sa_f	Sa_1	Sa_2	Sm	Sr	SA_{nv}	18	Ns_f	Sa_1	Sa_2	Sm	Sr	SA_{nv}
3	Sa_f	Sa_1	Sa_2	Lg	Wk	SA_{nv}	19	Ns_f	Sa_1	Sa_2	Lg	Wk	SA_{nv}
4	Sa_f	Sa_1	Sa_2	Lg	Sr	WA_{nv}	20	Ns_f	Sa_1	Sa_2	Lg	Sr	WA_{nv}
5	Sa_f	Sa_1	Ns_2	Sm	Wk	SA_{nv}	21	Ns_f	Sa_1	Ns_2	Sm	Wk	WA_{nv}
6	Sa_f	Sa_1	Ns_2	Sm	Sr	WA_{nv}	22	Ns_f	Sa_1	Ns_2	Sm	Sr	WR_{nv}
7	Sa_f	Sa_1	Ns_2	Lg	Wk	WA_{nv}	23	Ns_f	Sa_1	Ns_2	Lg	Wk	WR_{nv}
8	Sa_f	Sa_1	Ns_2	Lg	Sr	WR_{nv}	24	Ns_f	Sa_1	Ns_2	Lg	Sr	SR_{nv}
9	Sa_f	Ns_1	Sa_2	Sm	Wk	WA_{nv}	25	Ns_f	Ns_1	Sa_2	Sm	Wk	WR_{nv}
10	Sa_f	Ns_1	Sa_2	Sm	Sr	WA_{nv}	26	Ns_f	Ns_1	Sa_2	Sm	Sr	WR_{nv}
11	Sa_f	Ns_1	Sa_2	Lg	Wk	WR_{nv}	27	Ns_f	Ns_1	Sa_2	Lg	Wk	SR_{nv}
12	Sa_f	Ns_1	Sa_2	Lg	Sr	SR_{nv}	28	Ns_f	Ns_1	Sa_2	Lg	Sr	SR_{nv}
13	Sa_f	Ns_1	Ns_2	Sm	Wk	WA_{nv}	29	Ns_f	Ns_1	Ns_2	Sm	Wk	WR_{nv}
14	Sa_f	Ns_1	Ns_2	Sm	Sr	SR_{nv}	30	Ns_f	Ns_1	Ns_2	Sm	Sr	SR_{nv}
15	Sa_f	Ns_1	Ns_2	Lg	Wk	SR_{nv}	31	Ns_f	Ns_1	Ns_2	Lg	Wk	SR_{nv}
16	Sa_f	Ns_1	Ns_2	Lg	Sr	SR_{nv}	32	Ns_f	Ns_1	Ns_2	Lg	Sr	SR_{nv}

Table 3.2: The rule structure for new voice call request

Rule	P_f	P_{otg1}	P_{otg2}	$\$_{n+1}$	I_a	Z_{nd}	Rule	P_f	P_{otg1}	P_{otg2}	$\$_{n+1}$	I_a	Z_{nd}
1	Sa_f	Sa_1	Sa_2	*Sm*	*Wk*	SA_{nd}	17	Ns_f	Sa_1	Sa_2	*Sm*	*Wk*	SA_{nd}
2	Sa_f	Sa_1	Sa_2	*Sm*	*Sr*	SA_{nd}	18	Ns_f	Sa_1	Sa_2	*Sm*	*Sr*	SA_{nd}
3	Sa_f	Sa_1	Sa_2	*Lg*	*Wk*	WA_{nd}	19	Ns_f	Sa_1	Sa_2	*Lg*	*Wk*	WA_{nd}
4	Sa_f	Sa_1	Sa_2	*Lg*	*Sr*	WR_{nd}	20	Ns_f	Sa_1	Sa_2	*Lg*	*Sr*	WR_{nd}
5	Sa_f	Sa_1	Ns_2	*Sm*	*Wk*	WA_{nd}	21	Ns_f	Sa_1	Ns_2	*Sm*	*Wk*	WA_{nd}
6	Sa_f	Sa_1	Ns_2	*Sm*	*Sr*	WR_{nd}	22	Ns_f	Sa_1	Ns_2	*Sm*	*Sr*	SR_{nd}
7	Sa_f	Sa_1	Ns_2	*Lg*	*Wk*	WR_{nd}	23	Ns_f	Sa_1	Ns_2	*Lg*	*Wk*	SR_{nd}
8	Sa_f	Sa_1	Ns_2	*Lg*	*Sr*	SR_{nd}	24	Ns_f	Sa_1	Ns_2	*Lg*	*Sr*	SR_{nd}
9	Sa_f	Ns_1	Sa_2	*Sm*	*Wk*	WR_{nd}	25	Ns_f	Ns_1	Sa_2	*Sm*	*Wk*	WR_{nd}
10	Sa_f	Ns_1	Sa_2	*Sm*	*Sr*	WR_{nd}	26	Ns_f	Ns_1	Sa_2	*Sm*	*Sr*	SR_{nd}
11	Sa_f	Ns_1	Sa_2	*Lg*	*Wk*	WR_{nd}	27	Ns_f	Ns_1	Sa_2	*Lg*	*Wk*	SR_{nd}
12	Sa_f	Ns_1	Sa_2	*Lg*	*Sr*	SR_{nd}	28	Ns_f	Ns_1	Sa_2	*Lg*	*Sr*	SR_{nd}
13	Sa_f	Ns_1	Ns_2	*Sm*	*Wk*	WR_{nd}	29	Ns_f	Ns_1	Ns_2	*Sm*	*Wk*	SR_{nd}
14	Sa_f	Ns_1	Ns_2	*Sm*	*Sr*	SR_{nd}	30	Ns_f	Ns_1	Ns_2	*Sm*	*Sr*	SR_{nd}
15	Sa_f	Ns_1	Ns_2	*Lg*	*Wk*	SR_{nd}	31	Ns_f	Ns_1	Ns_2	*Lg*	*Wk*	SR_{nd}
16	Sa_f	Ns_1	Ns_2	*Lg*	*Sr*	SR_{nd}	32	Ns_f	Ns_1	Ns_2	*Lg*	*Sr*	SR_{nd}

Table 3.3: The rule structure for new data call request

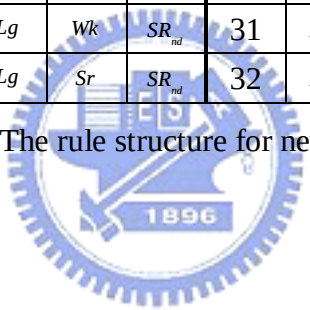

Rule	P_f	P_{otg1}	P_{otg2}	$\$_{n+1}$	Z_{hv}	Rule	P_f	P_{otg1}	P_{otg2}	$\$_{n+1}$	Z_{hv}
1	Sa_f	Sa_1	Sa_2	*Sm*	SA_{hv}	9	Ns_f	Sa_1	Sa_2	*Sm*	SA_{hv}
2	Sa_f	Sa_1	Sa_2	*Lg*	SA_{hv}	10	Ns_f	Sa_1	Sa_2	*Lg*	SA_{hv}
3	Sa_f	Sa_1	Ns_2	*Sm*	WR_{hv}	11	Ns_f	Sa_1	Ns_2	*Sm*	SA_{hv}
4	Sa_f	Sa_1	Ns_2	*Lg*	WR_{hv}	12	Ns_f	Sa_1	Ns_2	*Lg*	WA_{hv}
5	Sa_f	Ns_1	Sa_2	*Sm*	WR_{hv}	13	Ns_f	Ns_1	Sa_2	*Sm*	SA_{hv}
6	Sa_f	Ns_1	Sa_2	*Lg*	SR_{hv}	14	Ns_f	Ns_1	Sa_2	*Lg*	WA_{hv}
7	Sa_f	Ns_1	Ns_2	*Sm*	SR_{hv}	15	Ns_f	Ns_1	Ns_2	*Sm*	SR_{hv}
8	Sa_f	Ns_1	Ns_2	*Lg*	SR_{hv}	16	Ns_f	Ns_1	Ns_2	*Lg*	SR_{hv}

Table 3.4: The rule structure for handoff voice call request

Rule	P_f	P_{otg1}	P_{otg2}	$\hat{I}_{n+1}$	Z_{hv}	Rule	P_f	P_{otg1}	P_{otg2}	$\hat{I}_{n+1}$	Z_{hv}
1	Sa_f	Sa_1	Sa_2	*Sm*	SA_{hv}	9	Ns_f	Sa_1	Sa_2	*Sm*	SA_{hv}
2	Sa_f	Sa_1	Sa_2	*Lg*	SA_{hv}	10	Ns_f	Sa_1	Sa_2	*Lg*	SA_{hv}
3	Sa_f	Sa_1	Ns_2	*Sm*	WR_{hv}	11	Ns_f	Sa_1	Ns_2	*Sm*	SA_{hv}
4	Sa_f	Sa_1	Ns_2	*Lg*	WR_{hv}	12	Ns_f	Sa_1	Ns_2	*Lg*	WR_{hv}
5	Sa_f	Ns_1	Sa_2	*Sm*	WR_{hv}	13	Ns_f	Ns_1	Sa_2	*Sm*	SA_{hv}
6	Sa_f	Ns_1	Sa_2	*Lg*	SR_{hv}	14	Ns_f	Ns_1	Sa_2	*Lg*	WR_{hv}
7	Sa_f	Ns_1	Ns_2	*Sm*	SR_{hv}	15	Ns_f	Ns_1	Ns_2	*Sm*	SR_{hv}
8	Sa_f	Ns_1	Ns_2	*Lg*	SR_{hv}	16	Ns_f	Ns_1	Ns_2	*Lg*	SR_{hv}

Table 3.5: The rule structure for handoff data call request

Rule	$\hat{I}_{n+1}$	I_a	Z_r	Rule	$\hat{I}_{n+1}$	I_a	Z_r
1	*Sm*	*Wk*	*HR*	17	*Lg*	*Wk*	*BR*
2	*Sm*	*Sr*	*MR*	18	*Lg*	*Sr*	*BR*

Table 3.6: The rule structure for rate control at each burst

In *Layer 4*, the term set for the output linguistic variable of new voice call request $T(Z = Z_{nv})$ = {Straightly Accept, Weakly Accept, Weakly Reject, Straightly Reject}= { SA_{nv}, WA_{nv}, WR_{nv}, SR_{nv} }. Membership functions for Z_{nv} are denoted by $M(Z_{nv})$ ={ $m_{SA_{nv}}$, $m_{WA_{nv}}$, $m_{WR_{nv}}$, $m_{SR_{nv}}$ }, where $m_X(Z_{nv}) = f(Z_{nv}; X, 0, 0)$, and X is SA_{nv}, WA_{nv}, WR_{nv}, or SR_{nv}. The triangular function $f(x; x_0, a_0, a_1)$ is chosen to be the membership function and is given by

$$f(x; x_0, a_0, a_1) = \begin{cases} \dfrac{x - x_0}{a_0} + 1 & for \quad x_0 - a_0 < x \le x_0 \\ \dfrac{x_0 - x}{a_1} + 1 & for \quad x_0 < x \le x_0 + a_1 \\ 0 & otherwise \end{cases}, \tag{3.17}$$

where, as shown in Fig. 3.7, x_0 in $f(\cdot)$ is the center of the triangular function, and a_0 (a_1) is the left (right) width of the triangular function.

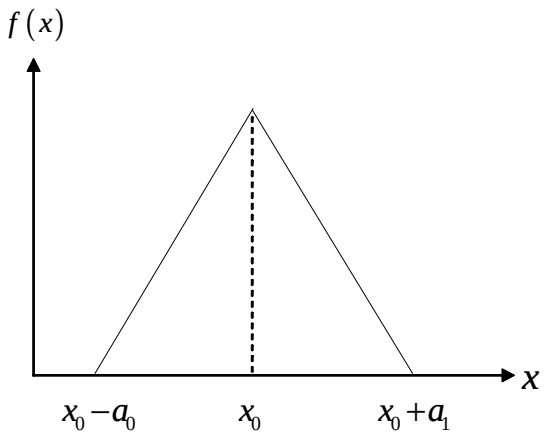

Figure 3.7: The figure of $f(\cdot)$

A new voice call request can be accepted if Z_{nv} is greater than an acceptance threshold z_{nva}, $SR_{nv} \le z_{nva} \le SA_{nv}$. Without a loss of generality, $SR_{nv} = 0$, $SA_{nv} = 1$, and let $WR_{nv} = (SR_{nv} + z_{nva})/2$, $WA_{nv} = (SA_{nv} + z_{nva})/2$. Similarly, the term set for the output linguistic variable of handoff voice call request $T(Z = Z_{hv})$ ={ SA_{hv}, WA_{hv}, WR_{hv}, SR_{hv} }, and membership functions for Z_{hv} are denoted by $M(Z_{hv})$ ={ $m_{SA_{hv}}$, $m_{WA_{hv}}$, $m_{WR_{hv}}$, $m_{SR_{hv}}$ }, where $m_X(Z_{hv}) = f(Z_{hv}; X, 0, 0)$, and X is SA_{hv}, WA_{hv}, WR_{hv}, or SR_{hv}. A handoff voice call request can be accepted if Z_{hv} is greater than an acceptance threshold z_{hva}, $SR_{hv} \le z_{hva} \le SA_{hv}$. Similarly, we set $SR_{hv} = 0$, $SA_{hv} = 1$, and let $WR_{hv} = (SR_{hv} + z_{hva})/2$, and $WA_{nv} = (SA_{nv} + z_{nva})/2$. And the term set for the output linguistic variable of data call request is similar as voice call request. The term set for the output linguistic variable of rate control $T(Z = Z_r)$ ={High Rate, Medium Rate, Basic Rate}={ HR, MR, BR }. Membership functions for Z_r are similar as what we mentioned before.

In *Layer 2* to *Layer 5*, the *max-min* inference method is adopted. The *max-min* inference method initially applies the *min* operator on membership values of terms of all input linguistic variables for each rule and then applies the *max* operator to yield the overall membership value, for each output term. For example, there are rule 3, rule 5, rule 19, and

rule 21 which have the same term WA_{nd} in table 3.3. Results of the *min* operator for rule 3, rule 5, rule 19, and rule 21, denoted as w_3, w_5, w_{19}, and w_{21}, are expressed as

$$w_3 = \min\left(m_{Sa_f}(P_f), m_{Sa_1}(P_{otg1}), m_{Sa_2}(P_{otg2}), m_{Lg}(\hat{I}_{n+1}), m_{Wk}(I_a) \right), \tag{3.18}$$

$$w_5 = \min\left(m_{Sa_f}(P_f), m_{Sa_1}(P_{otg1}), m_{Ns_2}(P_{otg2}), m_{Sm}(\hat{I}_{n+1}), m_{Wk}(I_a) \right), \tag{3.19}$$

$$w_{19} = \min\left(m_{Ns_f}(P_f), m_{Sa_1}(P_{otg1}), m_{Sa_2}(P_{otg2}), m_{Lg}(\hat{I}_{n+1}), m_{Wk}(I_a) \right), \tag{3.20}$$

$$w_{21} = \min\left(m_{Ns_f}(P_f), m_{Sa_1}(P_{otg1}), m_{Ns_2}(P_{otg2}), m_{Sm}(\hat{I}_{n+1}), m_{Wk}(I_a) \right). \tag{3.21}$$

Then, the method applies the *max* operator to yield the overall membership value of the term WA_{nd}, denoted as $w_{WA_{nd}}$, can be obtained by

$$w_{WA_{nd}} = \max(w_3, w_5, w_{19}, w_{21}). \tag{3.22}$$

The center of area defuzzification method is used because of its simplicity in computation. This defuzzification method obtains Z_{nd} by combining $w_{SA_{nd}}$, $w_{WA_{nd}}$, $w_{WR_{nd}}$, and $w_{SR_{nd}}$ as

$$Z_{nd} = \frac{w_{SA_{nd}} \times SA_{nd} + w_{WA_{nd}} \times WA_{nd} + w_{WR_{nd}} \times WR_{nd} + w_{SR_{nd}} \times SR_{nd}}{w_{SA_{nd}} + w_{WA_{nd}} + w_{WR_{nd}} + w_{SR_{nd}}}. \tag{3.23}$$

For Z_{nv}, Z_{hv}, Z_{hd}, and Z_r, the *max-min* inference method is employed to calculate the membership value and the center of area method is then applied for defuzzification, similarly.

For tuning the membership functions, different situations in the simulated WCDMA system are collected as training data. For example, $P_f(n)$, $P_{otg1}(n)$, $P_{otg2}(n)$, $\hat{I}_k(n+1)$ and $I_a(n)$ are recorded when a new call request arrives. This new call request will be accepted and the system recorded the home cell and adjacent cells' interferences at next time slot. The effect of these interferences, which are higher or lower than the threshold, is treated as the actual output of layer 5 and quantized to compare with the predicted output Q_5.

The output linguistic variables are single terms, which can reduce the complexity of the fuzzy models. So, $(p_i \times X + q_i \times Y + r_i)$ in equation (3.14) is set to be a constant, and the

max-min inference method can be implemented by ANFIS and the membership functions can be tuned.

By using the MATLAB fuzzy logic toolbox, ANFIS can be implemented efficiently. The *anfisedit* command is a graphical user interface (GUI) for editing ANFIS. This tool applies fuzzy inference techniques to data modeling. By using this ANFIS editor GUI, training data can be loaded and *anfisedit* adopts these training data to find the appropriate parameters. The shape of the membership functions depends on these parameters, and changing these parameters will change the shape of the membership functions. Using the given input/output data set, the toolbox function *anfisedit* constructs a fuzzy inference system whose membership function parameters are tuned using a backpropagation algorithm. After the system is fine-tuned, the membership functions are derived and they will be used in the neural fuzzy call admission and rate controller.

Chapter 4

Simulation Results and Discussion

In the simulations, we consider a WCDMA cellular system with $K = 49$ hexagonal cells, E_b/N_0 of type-1 connection $g_1^* = 7$ dB, E_b/N_0 of type-2 connection $g_2^* = 10$ dB, and the spreading factor of each basic code channel $SF = 256$. The air interface has the frame time of $T = 10$ m second, and the frequency spectrum bandwidth $W = 3.84$ MHz. The QoS requirements of outage probability are set to be $P_{otg1}^* = 2\times10^{-2}$ and $P_{otg2}^* = 5\times10^{-3}$, and the QoS constraint of forced termination probability is defined as $P_f^* = 5\times10^{-3}$.

To achieve the required outage requirement of type-2 connections, the processing gain ratio is chosen to be $R_G = R_2/R_1 = 3$, and therefore the SIR threshold before despreading are set to be $SIR_1^* = -14$ dB, $SIR_2^* = -17$ dB. The filtering factor (the exponential decay factor) to obtain the interference mean estimation is 0.02. The voice source model is assumed to be with $1/a = 1$ second and $1/b = 1.35$ seconds. If the data source is characterized by a batch Poisson process, the model is assumed to be with $1/A_d = 0.1$ and the size of data message is in a geometric distribution with mean 2 and maximum length 10. If the data source is characterized by a self-similar process and the packets are Pareto distributed, the model is assumed to be with $m_{N_{pc}} = 5$, $m_{D_{pc}} = 12$ seconds, $m_{N_p} = 25$, and $m_{D_p} = 0.0083$ second. The mean holding times for both voice and data services are 90 seconds. The speed of mobile users is either $V_1 = 20$ Km/Hr or $V_2 = 60$ Km/Hr with equal probability. The moving direction is modeled by the angle t with uniform distribution. The radio propagation parameters of q and z are set to be 4 and 8dB [21], [22], and the handoff margin is set to

be 3dB.

The effectiveness of the proposed neural fuzzy call admission and rate controller (NFCAC-RC) is tested by comparing it with the ICAC, which is proposed in [6]. Difference data source models will be considered individually in scenario one and two. In these two scenarios, the QoS requirements including the outage probability of type-1, the outage probability of type-2, and the forced termination probability will be examined to see if they are satisfactory. Then, the mean number of users and packets per second transmitted in a cell will be compared.

4.1 Scenario I: Data Source Model is Batch Poisson Distributed

In the first case, the data source model is characterized by a batch Poisson process. Neural fuzzy call admission controller (NFCAC), which is NFCAC-RC without rate control, is compared in this scenario, too. ICAC and NFCAC are compared with each other for their different input linguistic variables.

Fig. 4.1 shows the outage probabilities versus new call arrival rate for ICAC, NFCAC, and NFCAC-RC. It can be seen that all of them can guarantee the QoS requirements of outage probabilities for all traffic types in all arrival rate conditions. The lines of ICAC and NFCAC are almost overlapped with each other. The voice outage probability of NFCAC-RC is much smaller than those of ICAC and NFCAC before the new call arrival rate exceeding 0.5, and the curve of NFAC-RC is also smoothed out. This is because the rate control for data users reduces the system interference and decreases the outage probability of voice users. But rate control makes the ON state duration of data user increasing, which is the reason that P_{otg2} of NFCAC-RC is larger than the other two schemes.

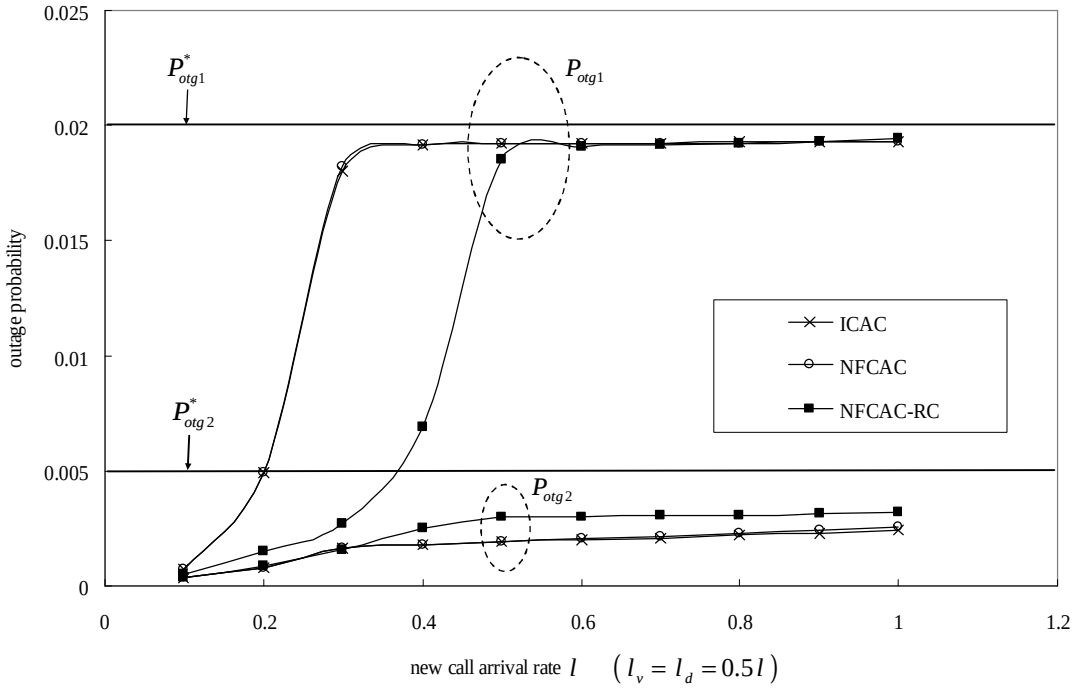

Figure 4.1: Outage probabilities versus new call arrival rate in scenario I

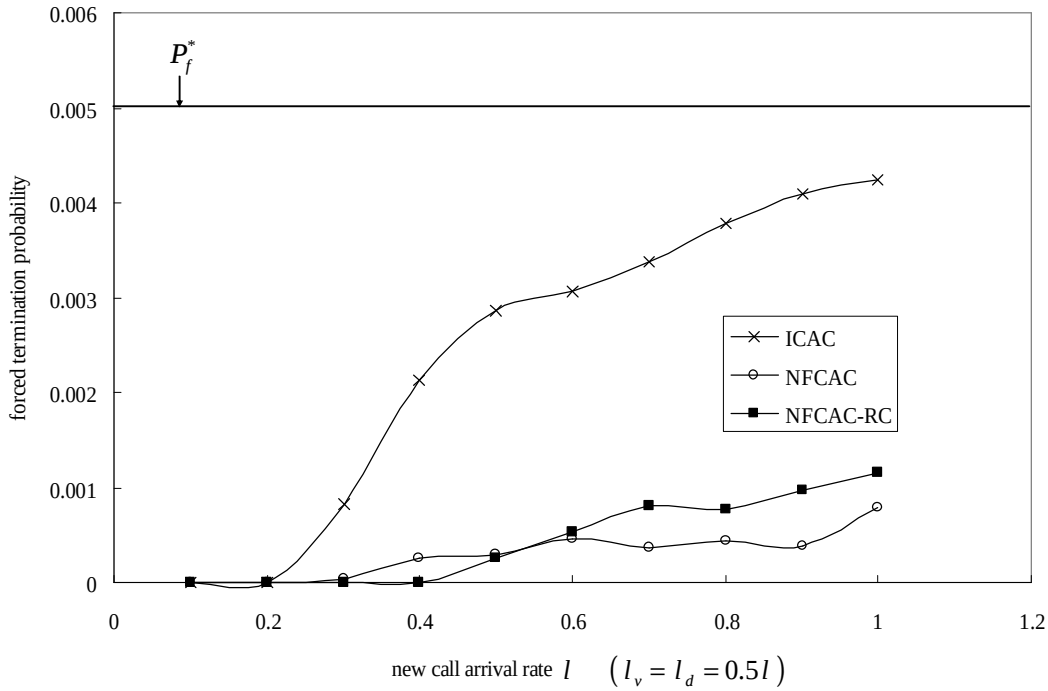

Figure 4.2: Forced termination probabilities versus new call arrival rate in scenario I

Fig. 4.2 shows the forced termination probabilities versus new call arrival rate for ICAC, NFCAC, and NFCAC-RC. Even though all of them guarantee the QoS requirements of forced termination probability, NFCAC and NFCAC-RC outperform ICAC significantly. By considering the influence of a call request on the adjacent cell base stations, NFCAC and NFCAC-RC reject new calls which are located near cell boundary when the system loading of adjacent cell is high. It will maintain the outage probability of adjacent cell not exceeding too high. According to the fuzzy rule of handoff call request, lower outage probability makes the handoff users be accepted more.

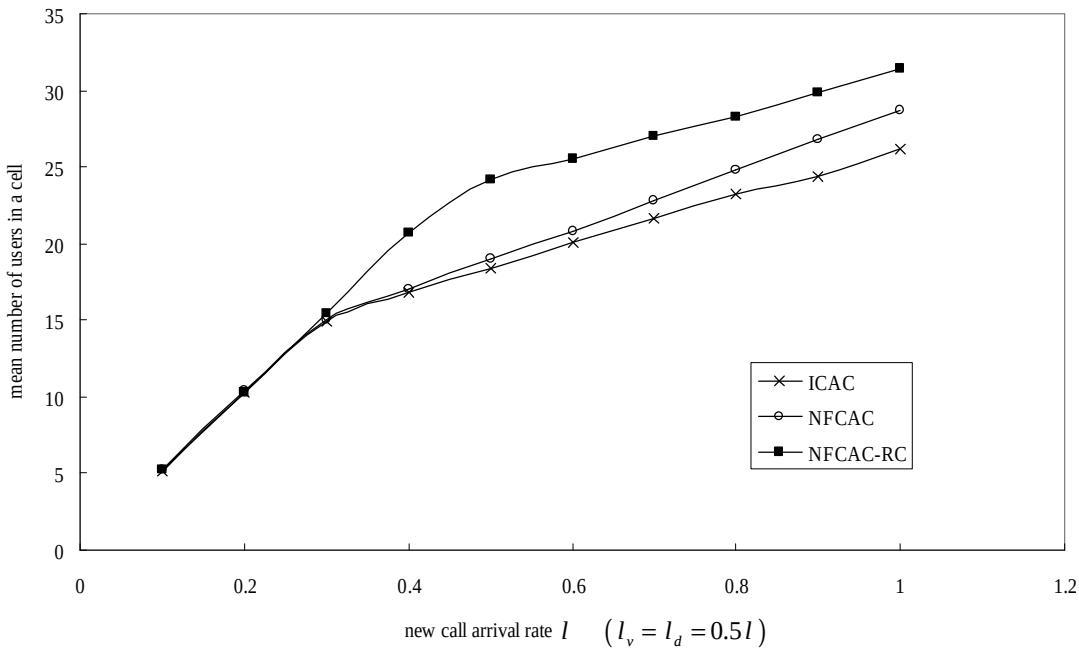

Figure 4.3: Mean number of users in a cell versus new call arrival rate in scenario I

Fig. 4.3 illustrates the mean number of users in a cell versus new call arrival rate for ICAC, NFCAC, and NFCAC-RC. It can be found that NFCAC-RC accepts users more than ICAC by an amount of 31.52%. Without rate control, NFCAC still accepts more number of users than ICAC by an amount of 9.53%. The rate control makes the data user not igniting

larger interference to the system and more users can be accepted. PRNN/ERLS interference predictor provides accuracy prediction and the system can accept user without exceeding the interference threshold.

Fig. 4.4 shows the mean packets per second transmitted in a cell versus new call arrival rate for ICAC, NFCAC, and NFCAC-RC. NFCAC-RC can attain maximal 50.81% compared with ICAC. Even without rate control, NFCAC improves about 4.53% more than ICAC. Such huge improvement in NFCAC-RC is because more users are accepted in the cell and data user with rate control will transmit for several time slots to finish the whole data.

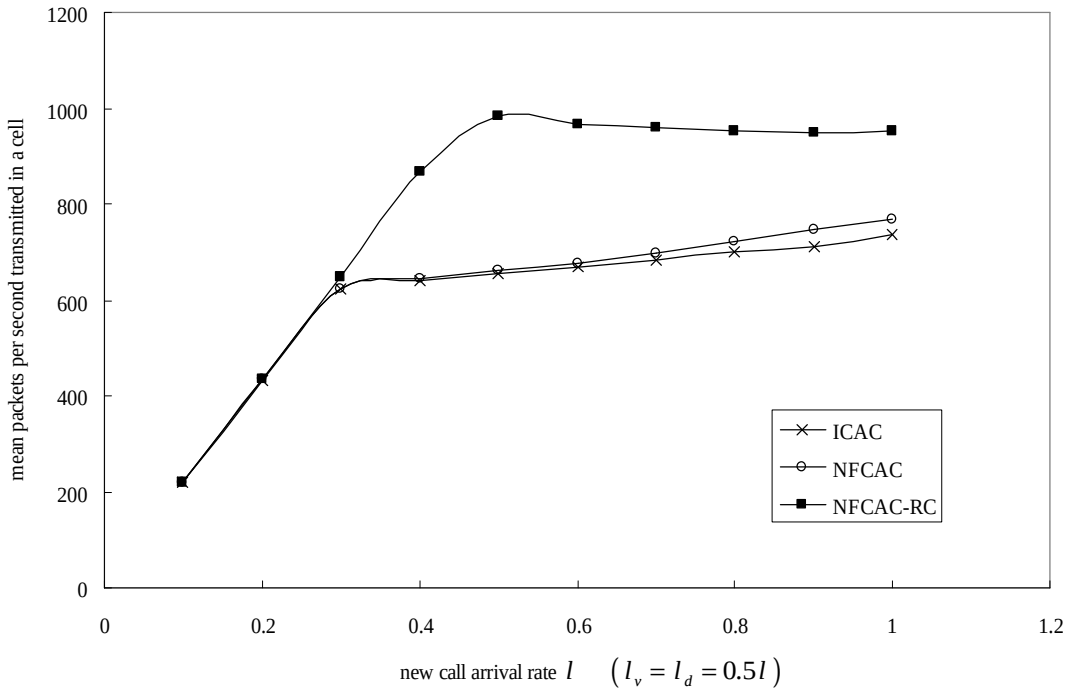

Figure 4.4: Mean packets per second transmitted in a cell versus new call arrival rate in scenario I

Fig. 4.5 illustrates the mean data packets delay time versus new call arrival rate for ICAC, NFCAC, and NFCAC-RC. According to the low-delay data defined as service class A

in [5], the delay-constraint is between 20 and 50ms. The mean data packets delay time of NFCAC-RC is 35ms and it is satisfied the constraint of low-delay data. The value of 35ms is set by the fuzzy rules and the membership functions of rate control. By tuning the membership functions, the delay time can be manipulated. For long constrained delay data and unconstrained delay data, the delay time of NFCAC-RC is satisfied, too. On the other hand, NFCAC and ICAC transmit data without delay.

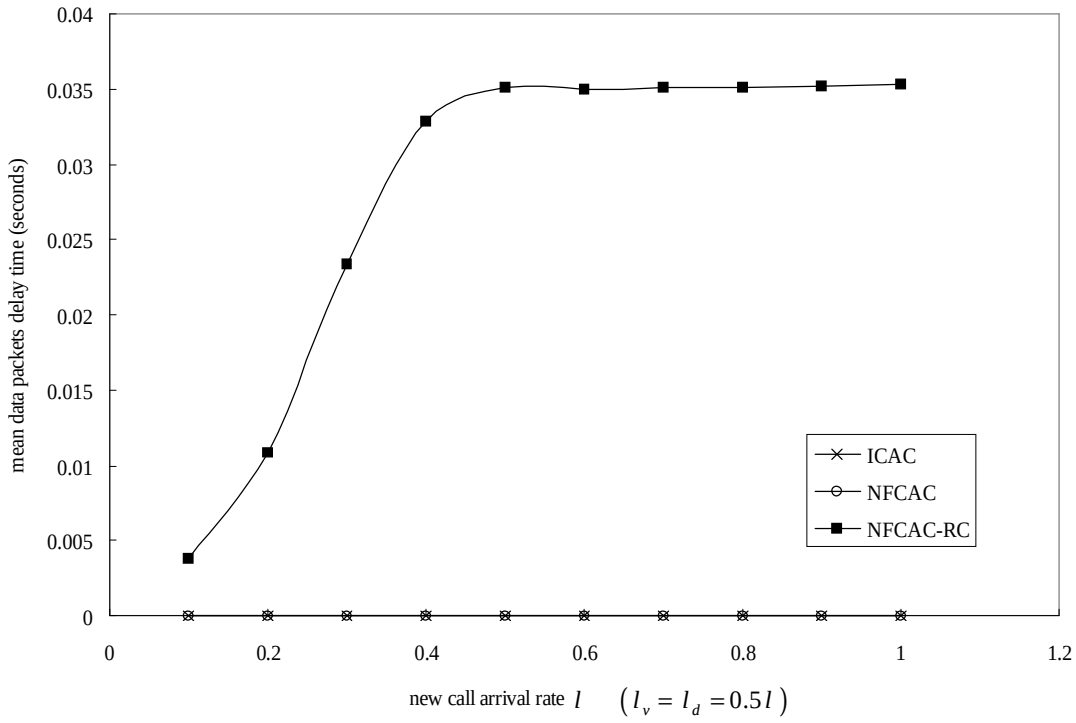

Figure 4.5: Mean data packets delay time versus new call arrival rate in scenario I

4.2 Scenario II: Data Source Model is Pareto Distributed

Then, we consider about the data source characterized by a self-similar process and the packets are Pareto distributed. By considering the bursty traffic condition, the capability of the CAC scheme could be tested.

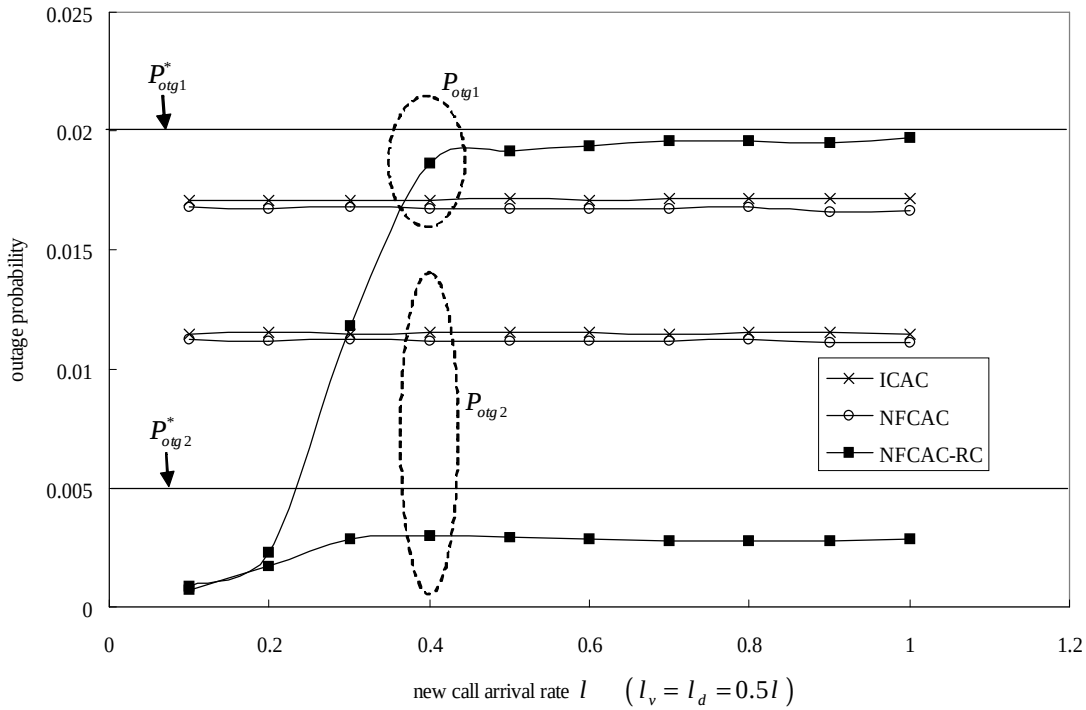

Figure 4.6: Outage probabilities versus new call arrival rate in scenario II

Fig. 4.6 shows the outage probabilities versus new call arrival rate for ICAC, NFCAC, and NFCAC-RC when the data packets are Pareto distributed. The data user generates bursty traffic and it causes the outage probability of type-2 out of order. Since the outage probability of type-2 is out of order, ICAC and NFCAC tend to reject new data call requests and handoff data call requests. Fewer data users in the system will lower the total interference so the outage probability of type-1 is reduced. NFCAC-RC can overcome this situation by adopting rate control on data users. Data traffic will not be so huge and the QoS requirements can be guaranteed. Even though NFCAC is not guaranteed the QoS requirement of the outage probability of type-2, the outage probabilities of NFCAC are better than ICAC's.

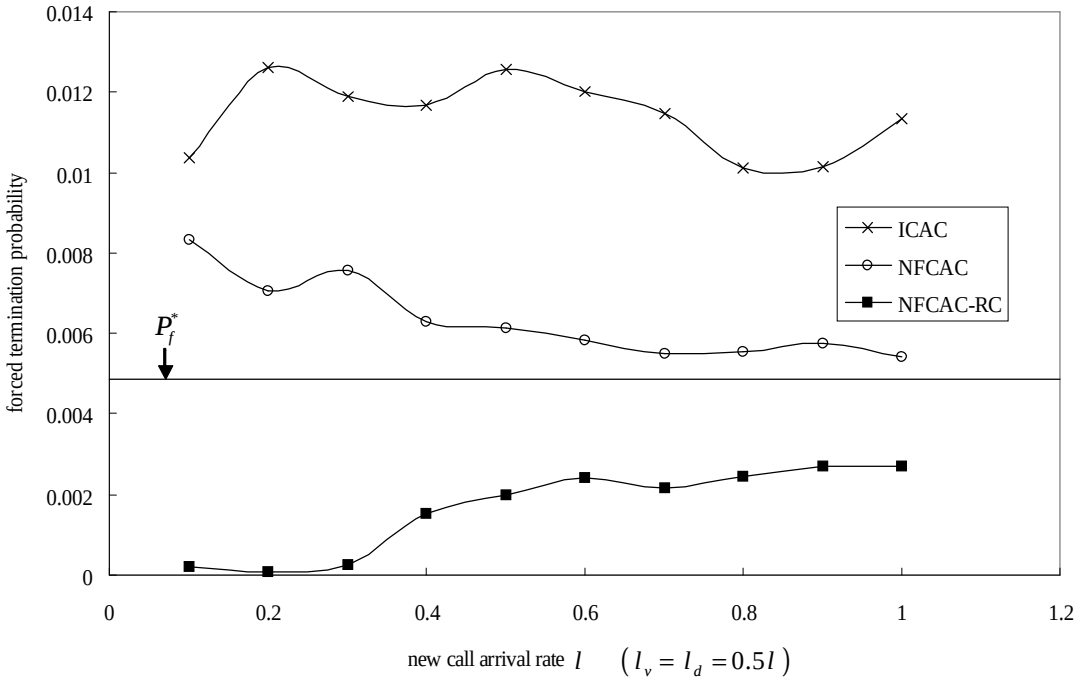

Figure 4.7: Forced termination probabilities versus new call arrival rate in scenario II

Fig. 4.7 shows the forced termination probabilities versus new call arrival rate for ICAC, NFCAC, and NFCAC-RC. For ICAC and NFCAC shown in Fig. 4.6, the outage probability of type-2 cannot guarantee the QoS requirement. According to the fuzzy rule of ICAC and NFCAC, it will reject the handoff call requests and the forced termination probability will increase. In Fig. 4.7, it can be seen that ICAC and NFCAC still cannot guarantee the QoS requirement of forced termination probability. On the other hand, NFCAC-RC does not experience the situation like ICAC and NFCAC, and the QoS requirements of forced termination probability can be guaranteed.

Fig. 4.8 illustrates the mean number of users in a cell versus new call arrival rate for ICAC, NFCAC, and NFCAC-RC. Notably, ICAC and NFCAC cannot guarantee the QoS requirements and most of the data users are rejected when the data packets are Pareto distributed. It can be seen that NFCAC-RC can still accept more users than ICAC by an amount of 114.70%. QoS requirements are input linguistic variables for fuzzy rules of ICAC,

NFCAC and NFCAC-RC. Since ICAC and NFCAC cannot guarantee the QoS requirements of outage probability of type-2 and forced termination probability, the fuzzy rule of ICAC and NFCAC tend to reject the call requests. The utilizations of ICAC and NFCAC are not efficient, and NFCAC-RC overcomes this situation.

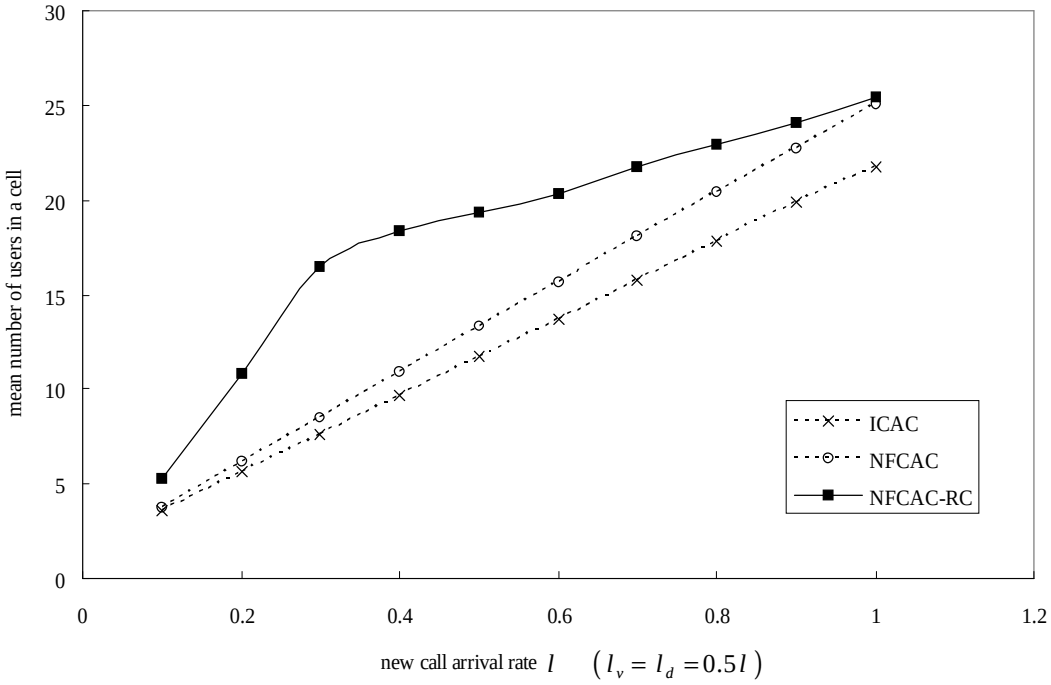

Figure 4.8: Mean number of users in a cell versus new call arrival rate in scenario II

In Fig. 4.8, it seems that the mean number of NFCAC is closed to NFCAC-RC when the arrival rate is increased. It is because NFCAC rejects data users and more voice users are in the system. Fig. 4.9 shows the mean number of voice and data users in a cell versus new call arrival rate for ICAC, NFCAC, and NFCAC-RC. The mean number of data users in ICAC and NFCAC are much smaller than NFCAC-RC. Even though the mean number of data users in ICAC and NFCAC are almost the same, the mean number of voice users in NFCAC is larger than ICAC.

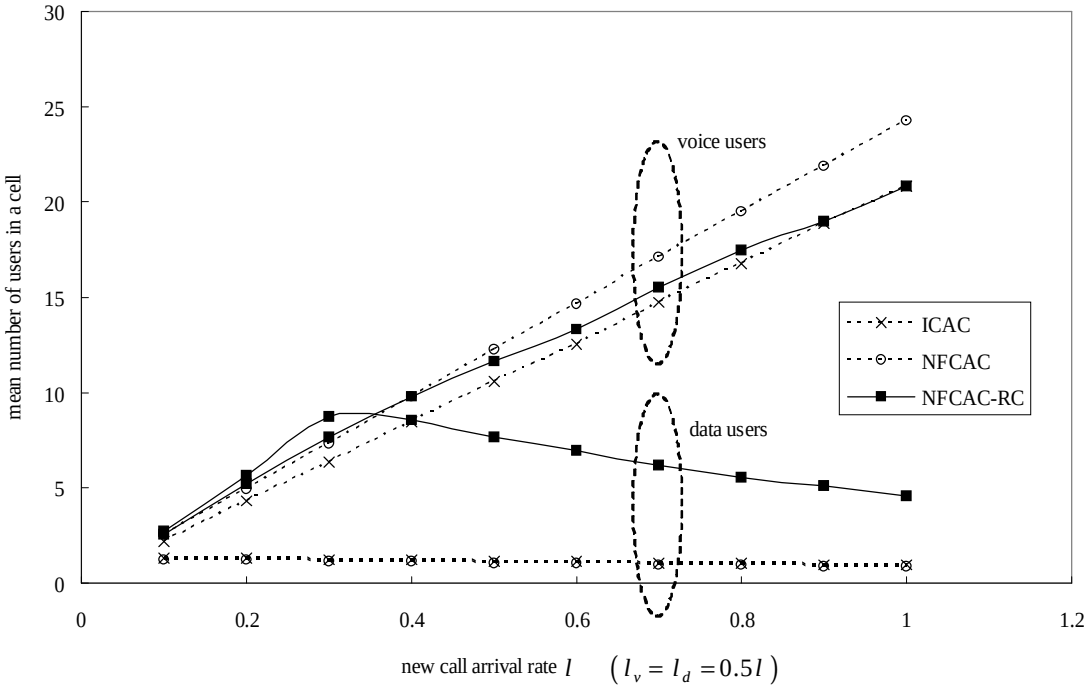

Figure 4.9: Mean number of voice and data users in a cell versus new call arrival rate in scenario II

Fig. 4.10 shows the mean packets per second transmitted in a cell versus new call arrival rate for ICAC, NFCAC, and NFCAC-RC. Although ICAC and NFCAC cannot guarantee the QoS requirements and most of the data users are rejected, NFCAC-RC can still attain maximal 254.96% compared with ICAC. After the new call arrival rate exceeding 0.3, the mean packets of NFCAC-RC are reduced. This situation can be explained that the data users increase and transmit many data packets at the new call arrival rate exceeding 0.3. The data packets are too many to be handled by the system, and the NFCAC-RC scheme tends to reject the new data call requests for maintaining the QoS requirements. The data users are reduced that cause this situation. In fact, scenario two is a strict situation for the system to serve data users transmitting huge packets. According to the simulation results, it can be seen that NFCAC-RC maintains the system QoS requirements, increases mean number of users in a cell by rate control scheme, and rejects heavily loading call requests when the system

cannot handle the situation.

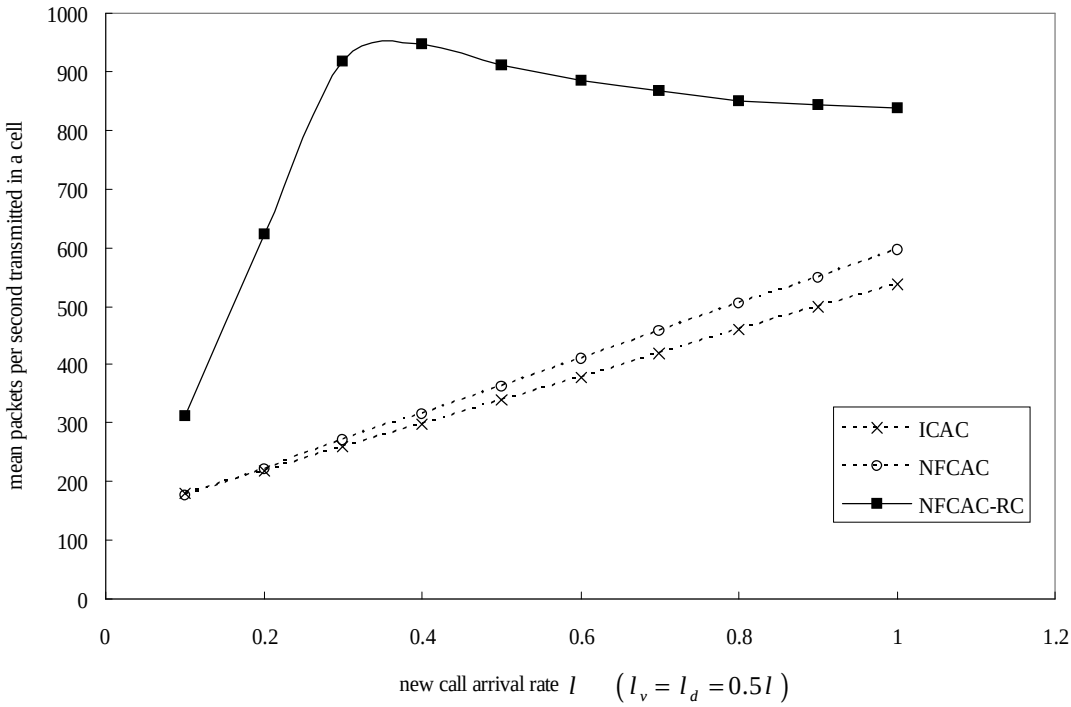

Figure 4.10: Mean packets per second transmitted in a cell versus new call arrival rate in scenario II

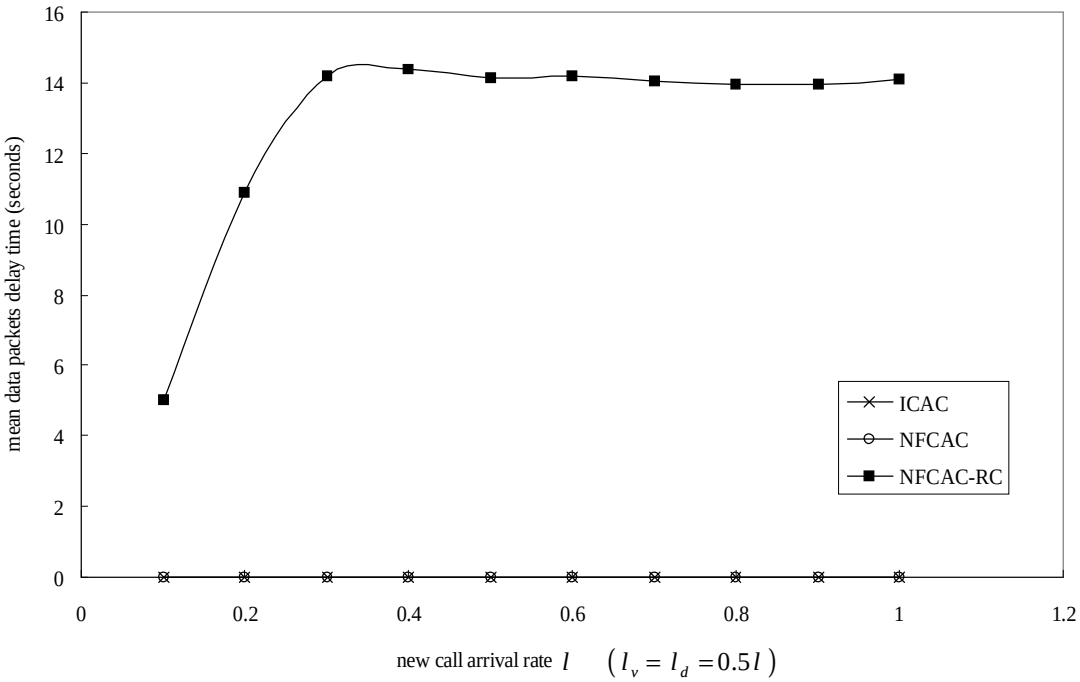

Figure 4.11: Mean data packets delay time versus new call arrival rate in scenario II

Fig. 4.11 illustrates the mean data packets delay time versus new call arrival rate for ICAC, NFCAC, and NFCAC-RC. In the scenario of bursty data traffic, the mean data packets delay time exceeds to 14 seconds. NFCAC-RC can maintain the QoS requirements of the best effort services. When the system is heavily loaded, all of the data users will transmit at basic rate and the delay time will increase. However, it is a trade-off between the system utilization and the delay time. In the scenario of bursty data traffic, it cannot be avoided to adopt rate control scheme. The membership functions of rate control in scenario two is the same as scenario one. If the delay time is a QoS requirement in the system, the membership functions of rate control should be changed to suit the scenario, or the delay time should be an input linguistic variable of the CAC scheme.

The system is much heavier in scenario two than in scenario one. ICAC and NFCAC cannot guarantee the QoS requirements when users transmit bursty data traffic. NFCAC-RC can overcome this situation by adopting rate control.

Chapter 5

Concluding Remarks

WCDMA cellular system has been shown to be an effective mobile system for personal communications. Due to the capacity of WCDMA is interference limited from all connected users, it is necessary to have an appropriate CAC scheme to manage the system resource. This thesis presents a neural fuzzy call admission and rate controller (NFCAC-RC) for WCDMA cellular systems to support differentiated QoS provisioning, satisfy the system QoS constraints, and maximize the system utilization.

By using the PRNN/ERLS interference predictor, NFCAC-RC forecasts the system interference at the next time period. It has been shown to achieve significantly higher prediction precision. The neural fuzzy call admission processor considers the system QoS performance measures of each traffic type and the interference of home cell and adjacent cells to determine whether to accept the call request or not. By using the MATLAB fuzzy logic toolbox, ANFIS can be implemented efficiently to fine-tune the membership functions. The neural network makes the fuzzy logic systems more adaptive and effective.

By considering the influence of a call request on the adjacent cell base stations, the CAC scheme becomes more precise. NFCAC-RC reduces the outage probability of adjacent cells, which is caused by accepting a new call request. New call requests, which are located near cell boundary, will be rejected when the system loading of adjacent cell is high. And the handoff call requests will be accepted more.

With rate control at each data burst, the mean number of users and mean packets in a cell are improved significantly. Considering the bursty traffic condition, the data source is

characterized by a self-similar process and the packets are Pareto distributed. According to the huge bursty traffic, ICAC cannot guarantee the outage probability of type-2 and the forced termination probability. To solve this problem, the rate control scheme has to be considered.

NFCAC-RC can guarantee the QoS requirements, maximize the mean number of users in a cell, and maximize the mean packets per second transmitted in a cell. Therefore, NFCAC-RC is suitable for WCDMA cellular systems.

Bibliography

[1] E. Dahlman, P. Beming, J. Knutsson, F. Ovesjo, M. Persson, and C. Roobol, "WCDMA—The radio interface for future mobile multimedia communications," *IEEE Trans. Veh. Technol.*, vol. 47, no. 4, pp. 1105-1118, Nov. 1998.

[2] H. Honkasalo, K. Pehkonen, M. T. Niemi, and A. T. Leino, "WCDMA and WLAN for 3G and beyond," *IEEE Wireless Commun.*, vol. 9, no. 2, pp. 14-18, Apr. 2002.

[3] Y. Ishikawa and N. Umeda, "Capacity design and performance of call admission control in cellular CDMA systems," *IEEE J. Select. Areas Commun.*, vol. 15, no. 8, pp. 1627-1635, Oct. 1997.

[4] S. M. Shin, C. H. Cho, and D. K. Sung, "Interference-based channel assignment for DS-CDMA cellular systems," *IEEE Trans. Veh. Technol.*, vol. 48, no. 1, pp. 233-239, Jan. 1999.

[5] N. Dimitriou and R. Tafazolli, "Quality of service for multimedia CDMA," *IEEE Commun. Mag.*, vol. 38, no. 7, pp. 88-94, July 2000.

[6] S. Shen, C. J. Chang, C. Y. Huang, and Q. Bi, "Intelligent call admission control for wideband CDMA cellular systems," *IEEE Trans. Wireless Commun.*, vol. 3, no. 5, pp. 1810-1821, Sept. 2004.

[7] J. S. Evans and D. Everitt, "Effective bandwidth-based admission control for multiservice CDMA cellular networks," *IEEE Trans. Veh. Technol.*, vol. 48, no. 1, pp. 36-46, Jan. 1999.

[8] M. E. Crovella and A. Bestavros, "Self-similarity in world wide web traffic: Evidence and possible causes," *IEEE/ACM Trans. Networking*, vol. 5, no. 6, pp. 835-846, Dec. 1997.

[9] H. Kang and K. Kim, "Throughput enhancement scheme for integrated voice/data DS-CDMA system: rate-based grouping transmission," *IEE Electron. Lett.*, vol. 35, no.

17, pp. 1437-1438, Aug. 1999.

[10] K. R. Lo, C. J. Chang, and C. B. Shung, "A neural fuzzy resource manager for hierarchical cellular systems supporting multimedia services," *IEEE Trans. Veh. Technol.*, vol. 52, no. 5, pp. 1196-1206, Sep. 2003.

[11] C. Comaniciu, N. B. Mandayam, D. Famolari, and P. Agrawal, "Wireless access to the world wide web in an integrated CDMA system," *IEEE Trans. Wireless Commun.*, vol. 2, no. 3, pp. 472-483, May 2003.

[12] J. Baltersee and J. A. Chambers, "Nonlinear adaptive prediction of speech with a pipelined recurrent neural network," *IEEE Trans. Signal Processing*, vol. 46, no. 8, pp. 2007-2216, Aug. 1998.

[13] J.-S. R. Jang, "ANFIS: adaptive-network-based fuzzy inference system," *IEEE Trans. Syst., Man, Cybern.*, vol. 23, no. 3, pp. 665-685, June 1993.

[14] L. Huang, S. Kumar, and C.-C. J. Kuo, "Adaptive resource allocation for multimedia QoS management in wireless networks," *IEEE Trans. Veh. Technol.*, vol. 53, no. 2, pp. 547-558, Mar. 2004.

[15] A. Adas, "Traffic models in broadband networks," *IEEE Commun. Mag.*, vol. 35, no. 7, pp. 82-89, July 1997.

[16] UMTS TR 101 112 V3.2.0 (1998-04), "Universal mobile telecommunications system; selection procedures for the choice of radio transmission technologies of the UMTS (UMTS 30.03 version 3.2.0)," *European Telecommunications Standards Institute, Tech. Rep.*, 1998.

[17] J. Zhang and W. Wang, "A dynamic channel allocation algorithm in TDD mode CDMA systems," *Proc. IEEE VTC Fall 2001*, vol. 1, pp. 385-388, 2001.

[18] Y. L. Hsieh, C. J. Chang, and Y. S. Chen, "A power control scheme with link gain prediction using PRNN/ERLS for DS-CDMA cellular mobile systems," *Proc. IEEE ICC '03*, vol. 1, pp. 407-411, May 2003.

[19] J.-S. R. Jang and C.-T. Sun, “Neuro-fuzzy modeling and control,” *Proc. IEEE*, vol. 83, no. 3, pp. 378-406, Mar. 1995.

[20] J.-S. R. Jang, C.-T. Sun, and E. Mizutani, Neuro-fuzzy and soft computing, Prentice-Hall, 1997.

[21] K. S. Gilhousen, I. M. Jacobs, R. Padovani, A. J. Viterbi, L. A. Weaver, Jr., and C. E. Wheatley III, “On the capacity of a cellular CDMA system,” *IEEE Trans. Veh. Technol.*, vol. 40, no. 2, pp. 303-312, May 1991.

[22] A. J. Viterbi, A. M. Viterbi, K. S. Gilhousen, and E. Zehavi, “Soft handoff extends CDMA cell coverage and increases reserve link capacity,” *IEEE J. Select. Areas Commun.*, vol. 12, no. 8, pp. 1281-1288, Oct. 1994.

Vita

姓名：郭立忠

學歷：

2003 ~ 2005 國立交通大學電信工程研究所

1995 ~ 1999 國立台灣大學電機工程學系

1992 ~ 1995 國立武陵高級中學

E-mail: lckuo.cm92g@nctu.edu.tw